Rigorous Asymptotic Models of Water Waves

Arthur Cheng

Department of Mathematics National Central University Jhongli, Taoyuan 32001 Taiwan email: cchsiao@math.ncu.edu.tw

Rafael Granero-Belinchón

Departamento de Matemáticas, Estadística y Computación Universidad de Cantabria Santander, España email: rafael.granero@unican.es

Steve Shkoller

Department of Mathematics University of California Davis, CA 95616 USA email: shkoller@math.ucdavis.edu

Jon Wilkening

Department of Mathematics University of California Berkeley, CA 94720 USA email: wilken@math.berkeley.edu

November 22, 2018

Abstract. We develop a rigorous asymptotic derivation of two mathematical models of water waves that capture the full nonlinearity of the Euler equations up to quadratic and cubic interactions, respectively. Specifically, letting ϵ denote an asymptotic parameter denoting the steepness of the water wave, we use a Stokes expansion in ϵ to derive a set of linear recursion relations for the tangential component of velocity, the stream function, and the water wave parameterization. The solution of the water waves system is obtained as an infinite sum of solutions to linear problems at each $O(\epsilon^k)$ level, and truncation of this series leads to our two asymptotic models, which we call the quadratic and cubic h-models.

These models are well-posed in spaces of analytic functions. We prove error bounds for the difference between solutions of the h-models and the water waves system. We also show that the Craig-Sulem models of water waves can be obtained from our asymptotic procedure.

We then develop a novel numerical algorithm to solve the quadratic and cubic h-models as well as the full water waves system. For three very different examples, we show that the agreement between the model equations and the water waves solution is excellent, even when the wave steepness is quite large. We also present a numerical example of corner formation for water waves.

Contents

1	Intr	roduction	2
2	Son	ne notation and definitions	4
	2.1	Matrix indexing	4
	2.2	Power series summation	Ę
	2.3	The water wave parameterization	Ę
	2.4	The fluid domain and some geometric quantities	Ę
		Derivatives	
	2.6	Fourier series	6
	2.7	Singular integral operators	6
		2.7.1 Function spaces	6

3	Water waves equations	7
	3.1 The Bernoulli equation	7
	3.2 The evolution of the tangential velocity	7
	3.3 The equation for the stream function	9
	3.4 The evolution equation for the free-surface	9
4	Stokes expansion and linear recursion for the time-dependent water waves	10
	4.1 Stokes expansion	10
	4.2 Linear recursion for the stream function	10
	4.3 Linear recursion for the height function	11
	4.4 Linear recursion for the tangential velocity	11
5	Derivation of the quadratic and cubic h-models	12
	5.1 Preliminary lemmas	12
	5.2 The quadratic h -model	14
	5.3 The quadratic h -model with surface tension	17
	5.4 The cubic h -model	17
6	Well-posedness of the h-models	23
	6.1 Well-posedness theory for the quadratic h -model	24
	6.2 Well-posedness theory for the cubic h -model	24
7	The Craig-Sulem $WW2$ model	27
8	Estimating the difference between the h -models and the solution of the full water	
	waves problem	2 9
9	Numerical comparison of water waves and the h-model	31
	9.1 Solving the Euler equations	31
	9.2 Timestepping the h -model	32
	9.3 Comparison of water waves and the h -model	35
	9.4 Conclusions from our simulations	43
A	Basic commutator identities	44
В	Another proof of Theorem 3	44

1 Introduction

Both gravity and capillary water waves are modeled by the free-surface incompressible Euler equations of fluid dynamics, and for many applications, the fluid is additionally assumed to be irrotational. Well-posedness, stability, and singularity formation have been well studied with many results; see, for example, [60, 83, 30, 14, 12, 80, 81, 82, 8, 50, 52, 26, 73, 24, 22, 6, 44, 37, 46, 45, 7, 20, 27, 35, 28, 32]. However, the Euler equations are sufficiently complicated that for many physical scenarios, a precise understanding of the dynamics of the solutions to the full water waves problem is not (at this time) known. Consequently, since the pioneering works of Airy, Boussinesq and Stokes [1, 17, 18, 76], there has been a sustained effort to find suitable approximations of the Euler equations, specific to certain asymptotic regimes. Such approximate asymptotic models have closely related dynamics

and can be significantly easier to analyze. Herein, we develop an asymptotic procedure that yields approximate model equations for the water waves problem to various orders of approximation of the nonlinearity. In particular, we present two models that respectively capture the nonlinearity up to quadratic and cubic interactions.

We derive two asymptotic models for the evolution of both gravity and gravity-capillary waves in deep water, using an asymptotic expansion in the steepness of the wave ϵ , which we view as a small parameter, equivalent to the ratio of the amplitude to the wavelength. Such an expansion has been used extensively since it was introduced by Stokes [76]; see, for example, [3, 61, 62, 4, 5]). Starting with the case of gravity water waves, we employ such a Stokes expansion and obtain linear recursion relations for the stream function, the tangential component of velocity, and the free-surface parameterization. Truncating this expansion to $O(\epsilon^3)$ yields a quadratic model equation for gravity water waves. We refer to this PDE as the quadratic h-model

$$\partial_t^2 h + g\Lambda h = -\Lambda(|H\partial_t h|^2) + g\Lambda(h\Lambda h) + g\partial_1(h\partial_1 h). \tag{1}$$

Keeping all terms in the recursion relation to $O(\epsilon^4)$ yields the *cubic h-model*, a new model of water wave dynamics that accurately captures the cubic interactions of the Euler equations and is given by

$$\partial_t^2 h + g\Lambda h = -\Lambda [(H\partial_t h)^2] + g\partial_1 (h\partial_1 h) + g\Lambda (h\Lambda h) + Q(h)$$
(2)

where the cubic nonlinearity Q(h) is defined in (63). Asymptotic models for gravity-capillary waves are derived in the same fashion (in section 5.3) when gravity and surface tension forces are of the same order.

The same expansion procedure that we used for the one-fluid problem can be used to derive models for two-fluid internal waves and the Rayleigh-Taylor instability (as noted in Remark 2 below). Furthermore, our approach can be applied to the case of finite-depth fluids as well.

We note that the quadratic h-model was derived using very different approaches by Matsuno [53, 54, 55] and later by Akers & Milewski [2]. The cubic h-model was also written down in the appendix of [54]. See also the papers of Benney & Luke [15], Choi [25], Lannes & Bonneton [51], Berger & Milewski [16], Akers & Nicholls [3], and Granero & Shkoller [38] for derivations of related models of water waves.

We show that both the quadratic and cubic h-models are well-posed in spaces of analytic functions that are similar to the Wiener algebra but with a (growing) exponential weight (used to guarantee analyticity). Well-posedness of the quadratic h-model follows from an application of the Cauchy-Kowalewski theorem, while the well-posedness of the cubic h-model is established using a slightly different approach¹, wherein we prove the summability of the Stokes expansion by obtaining bounds for our linear recursion, which can be estimated in terms of the Catalan numbers [75] from number theory.

 $^{^{1}}$ It is likely that well-posedness of the cubic h-model follows also from an application of the Cauchy-Kowalewski theorem once certain reductions of the cubic nonlinearity are established, but we did not pursue this direction.

We also establish rigorous error bounds for the difference between solutions of the h-models and the full water waves system. We thus conclude that both the quadratic and cubic h-models are accurate asymptotic models of water waves in the small ϵ -regime.

The asymptotic procedure that we shall describe below allows us to derive a large class of asymptotic models of water waves, including the well-known hierarchy of models obtained by Craig & Sulem [31]; in particular, we show that their most studied model, WW2 (or water waves 2), is obtained from our approach. Moreover, we write the WW2 model as a second-order wave equation and explain its connection with the quadratic h-model.

Finally, we present an arbitrary-order exponential time differencing scheme [29, 48, 21] for solving the quadratic and cubic h-models accurately and efficiently and compare those solutions against numerical solutions of the Euler equations. We show that the h-models converge as expected: with ϵ denoting the maximum slope of the initial condition, the quadratic and cubic h-models converge in L^2 to solutions of the full water waves problem with rates $O(\epsilon^2)$ and $O(\epsilon^3)$, respectively, where the L^2 error is scaled by ϵ^{-1} to account for the decreasing (as a function of ϵ) norm of the exact solution. We give three examples of initial data that show excellent agreement between the h-models and the full water waves solution all the way up to $\epsilon = O(1)$. The first example is a multi-hump initial condition in which a jet forms in each trough as the solution drops from rest; the second example is a localized disturbance over a flat surface that propagates outward as time evolves; and the third example is a family of standing water waves. In all three cases, the quadratic and cubic models are much better than linear theory at capturing features of the dynamics. For large ϵ , the quadratic model has a tendency to form a corner singularity while the cubic model tracks the Euler solution quite well. We also present a continuation of the first example for the Euler equations to show that the wave eventually overturns and appears to form a corner singularity before self-intersecting, with $dP/dn \to 0$ at the tip of one of the overturning waves.

Paper Outline. In Section 2, we introduce the notation and some important definitions used throughout the paper. In Section 3, we introduce the water waves equations, and the three fundamental variables that shall be evolved: the tangential component of velocity, the stream function, and the free-surface parameterization. Section 4 is devoted the Stokes expansion of the water waves system and the derivation of the linear recursion relations. In Section 5, we derive the quadratic and cubic h-models, and in Section 6, we prove that these models are well-posed. In Section 7, we derive the Craig-Sulem WW2 model, and prove that it too is well-posed. Section 8 establishes the error estimates for solutions of the h-models compared to the full water waves system. Then, in Section 9, we perform a number of numerical experiments that compare the quadratic and cubic h-models with a highly accurate numerical solution of the full water waves system.

2 Some notation and definitions

2.1 Matrix indexing

Let A be a matrix, and b be a column vector. Then, we write A_j^i for the component of A, located on row i and column j; consequently, using the Einstein summation convention, we

write

$$(Ab)^k = A_i^k b^i$$
 and $(A^T b)^k = A_k^i b^i$.

2.2 Power series summation

We adopt the convention that independent of the summand s_i ,

$$\sum_{j=0}^{k-\ell} s_j = 0 \quad \text{whenever } k < \ell \,. \tag{3}$$

2.3 The water wave parameterization

We identify \mathbb{S}^1 with the interval $[-\pi, \pi]$. We shall denote a general parameterization of the free-surface of the fluid by the diffeomorphism $z(\cdot, t) : \mathbb{S}^1 \to \mathbb{R}^2$. This free-surface of the fluid is the water wave, which we denote by $\Gamma(t)$. Hence, the water wave is given by

$$\Gamma(t) = \{ (z_1(x_1, t), z_2(x_1, t)) : -\pi \leqslant x_1 \leqslant \pi, \ t \in [0, T] \}.$$

For the majority of our analysis, we shall assume that the water wave evolves as a graph over the horizontal x_1 -axis. in particular, $(z_1, z_2) = (x_1, h(x_1, t))$ and

$$\Gamma(t) = \{ (x_1, h(x_1, t)) : -\pi \leqslant x_1 \leqslant \pi, \ t \in [0, T] \}.$$
(4)

The one-to-one function $h(x_1,t)$ is often called the signed height function.

2.4 The fluid domain and some geometric quantities

The time-dependent fluid domain is defined as

$$\Omega(t) = \{ (x_1, x_2) : -\pi \leqslant x_1 \leqslant \pi, -\infty \leqslant x_2 \leqslant z_2(x_1, t), \ t \in [0, T] \},$$
 (5)

i.e. for the sake of simplicity, we assume that the depth of the fluid is much larger than the amplitude of the wave.

We define the reference domain \mathcal{D} as

$$\mathcal{D} = \mathbb{S}^1 \times (-\infty, 0). \tag{6}$$

We let $\mathbf{N} = \mathbf{e}_2$ denote the outward unit normal to $\partial \mathcal{D}$, and we let $\boldsymbol{\tau}(\cdot,t)$ and $\boldsymbol{\kappa}(\cdot,t)$ denote, respectively, the unit tangent and normal vectors to the water wave $\Gamma(t)$, where $\boldsymbol{\kappa}(\cdot,t)$ points outward to the set $\Omega(t)$. We then set

$$n = \mathcal{N} \circ z$$
 and $\tau = \tau \circ z$.

When the water wave is defined by graph parameterization (4), the induced metric g is given by

$$g = 1 + (\partial_1 h)^2. (7)$$

2.5 Derivatives

We write

$$\partial_k f = \frac{\partial f}{\partial x_k}$$
 for $k = 1, 2$, $\partial_t f = \frac{\partial f}{\partial t}$, $\nabla = (\partial_1, \partial_2)$, $\nabla^{\perp} = (-\partial_2, \partial_1)$,

and for a vector F,

$$\operatorname{div} F = \nabla \cdot F \text{ and } \operatorname{curl} F = \nabla^{\perp} \cdot F.$$

The Laplace operator is defined as $\Delta = \partial_1^2 + \partial_2^2$.

2.6 Fourier series

If $f: \mathbb{S}^1 \to \mathbb{R}$ is a square-integrable 2π -periodic function, then it has the Fourier series representation $f(x_1) = \sum_{k=-\infty}^{\infty} \hat{f}(k)e^{ikx_1}$ for all $x_1 \in \mathbb{S}^1$, where the complex Fourier coefficients are defined by $\hat{f}(k) = \frac{1}{2\pi} \int_{\mathbb{S}^1} f(x_1)e^{-ikx_1}dx_1$. We shall sometimes write \hat{f}_k for $\hat{f}(k)$. Functions $g: \mathcal{D} \to \mathbb{R}$ (which are square-integrable in x_1 can be expanded as $g(x_1, x_2) = \sum_{k \in \mathbb{Z}} \hat{g}(x_2, k)e^{ikx_1}$ for all $(x_1, x_2) \in \mathcal{D}$, where $\hat{g}(x_2, k) = \frac{1}{2\pi} \int_{\mathbb{S}^1} g(x_1, x_2)e^{-ikx_1}dx_1$.

2.7 Singular integral operators

Let $f(x_1)$ denote a 2π periodic function on \mathbb{S}^1 . Using the Fourier representation, we define the Hilbert transform H and the Dirichlet-to-Neumann operator Λ as

$$\widehat{Hf}(k) = -i\operatorname{sgn}(k)\widehat{f}(k), \quad \widehat{\Lambda f}(k) = |k|\widehat{f}(k).$$
 (8)

In particular, we note that

$$\partial_1 H = \Lambda, \quad H^2 = -1.$$

Equivalently, suppose that $f: \mathbb{S}^1 \to \mathbb{R}$ is a 2π periodic function and that Φ is its harmonic extension to \mathcal{D} . Then,

$$\Lambda f = \partial_2 \Phi \quad \text{on} \quad \mathbb{S}^1 \times \{0\} \,. \tag{9}$$

Finally, we denote the commutator between f and the Hilbert transform acting on g as

$$[\![H,f]\!]g = H(fg) - fHg.$$

Let us observe that $[\![f,H]\!]g = -[\![H,f]\!]g$.

2.7.1 Function spaces

For $1 , we denote by <math>L^p(\mathbb{S}^1)$ the set of Lebesgue measurable 2π -periodic functions such that $\|u\|_{L^p} < \infty$ where $\|u\|_{L^p} = \left(\int_{\mathbb{S}^1} |u(x)|^p dx\right)^{\frac{1}{p}}$ if $1 and <math>\|u\|_{L^\infty} = \int_{\mathbb{S}^1} |u(x)|^p dx$

ess $\sup_{x \in \mathbb{S}^1} |u(x)|$. For integers $k \ge 0$, we let $H^k(\mathbb{S}^1) = \left\{ u : L^2(\mathbb{S}^1) \mid \|u\|_{H^k}^2 := \sum_{i=0}^k \|\partial_1^j u\|_{L^2} < 1 \right\}$ ∞ \}. For $s \in \mathbb{R}$, we then define the space $H^s(\mathbb{S}^1)$ to be the 2π -periodic distributions such that $||u||_{H^s}^2 := \sum_{m=-\infty}^{\infty} (1+m^2)^s |\hat{u}_m|^2 < \infty.$

For a given $\tau > 0$, we define the following Banach scale of analytic functions as

$$X_{\tau} = \left\{ u : \mathbb{S}^1 \to \mathbb{R} \,\middle|\, \|f\|_{X_{\tau}} = \sum_{m \in \mathbb{Z}} e^{\tau |m|} |\hat{u}_m| < \infty \right\}. \tag{10}$$

$\mathbf{3}$ Water waves equations

Water waves are modeled by the incompressible and irrotational free-surface Euler equations, written as

$$\partial_t \mathbf{u} + (\mathbf{u} \cdot \nabla) \mathbf{u} + \nabla p = \mathbf{0}$$
 in $\Omega(t)$, (11a)

$$\operatorname{curl} \boldsymbol{u} = \operatorname{div} \boldsymbol{u} = 0 \qquad \qquad \text{in} \quad \Omega(t) \,, \tag{11b}$$

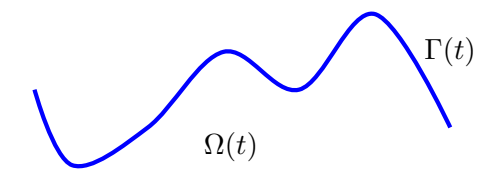
$$p = -\lambda \frac{\partial_1^2 h}{(1 + (\partial_1 h)^2)^{3/2}} \quad \text{on} \quad \Gamma(t),$$

$$\mathbf{u} = \mathbf{u}_0 \quad \text{on} \quad \Omega \times \{t = 0\},$$
(11b)

$$\mathbf{u} = \mathbf{u}_0 \qquad \qquad \text{on} \quad \Omega \times \{t = 0\}, \tag{11d}$$

$$\mathcal{V}(\Gamma(t)) = \boldsymbol{u} \cdot \boldsymbol{\mathcal{N}}, \tag{11e}$$

where $t \in [0, T]$, $\Omega(t)$ is defined in (5), $\Gamma(t)$ is defined in (4), $0 \le \lambda$ is the surface tension parameter and $\mathcal{V}(\Gamma(t)) = \boldsymbol{u} \cdot \boldsymbol{\mathcal{N}}$ means that the free-surface $\Gamma(t)$ moves with normal velocity $\boldsymbol{u} \cdot \boldsymbol{\mathcal{N}}$. We shall assume that all functions are 2π -periodic in x_1 .



3.1 The Bernoulli equation

Since $\operatorname{curl} \boldsymbol{u} = 0$ in $\Omega(t)$, $\boldsymbol{u} = \nabla \phi$ for some scalar potential ϕ . Then, (11a) can be written as

$$\partial_t \phi(x,t) + \frac{1}{2} |\nabla \phi(x,t)|^2 + p(x,t) + \rho g x_2 = f(t) \quad \forall x \in \Omega(t) \text{ and } t > 0.$$
 (12)

where f is a function independent of x.

3.2The evolution of the tangential velocity

On \mathbb{S}^1 , we define the following quantities:

$$v = u \circ z$$
, $\Psi = \phi \circ z$, and $n = \mathcal{N} \circ z$.

We shall make use of the tangential velocity

$$\omega = \boldsymbol{u} \cdot \boldsymbol{\tau}$$
 and $\bar{\omega}(x_1, t) = \boldsymbol{v}(x_1, t) \cdot \partial_1 z(x_1, t)$ on $\Gamma(t)$.

From (11e), $\partial_t z \cdot \boldsymbol{n} = \boldsymbol{v} \cdot \boldsymbol{n}$ so that

$$\partial_t z(x_1, t) = \mathbf{v}(x_1, t) + c(x_1, t)\partial_1 z(x_1, t) \tag{13}$$

for an arbitrary scalar function c. (Note that $\partial_1 z$ is a tangent vector and that the water waves problem has a tangential reparameterization symmetry.)

By the chain rule,

$$\partial_1 \Psi(x_1, t) = \partial_1 z(x_1, t) \cdot (\nabla \phi) \circ z(x_1, t) = (\boldsymbol{v} \cdot \partial_1 z)(x_1, t) = \overline{\omega}(x_1, t), \tag{14}$$

and

$$\partial_t \Psi(x_1, t) = \partial_t \phi(z(x_1, t), t) + \partial_t z(x_1, t) \cdot (\nabla \phi) \circ z(x_1, t)$$

= $(\partial_t \phi \circ z + \partial_t z \cdot \mathbf{v})(x_1, t)$.

From (14), $\partial_1 \partial_t \Psi(x_1, t) = \partial_t \overline{\omega}(x_1, t)$, and (13) shows that

$$\partial_t \Psi(x_1,t) = (\partial_t \phi \circ z)(x_1,t) + |\boldsymbol{v}(x_1,t)|^2 + c(x_1,t)\,\bar{\omega}(x_1,t).$$

Therefore, we find that $\bar{\omega}$ satisfies

$$\partial_t \bar{\omega} = \partial_1 \left(\partial_t \phi \circ z + |\mathbf{v}|^2 + c \,\bar{\omega} \right). \tag{15}$$

From (12),

$$(\partial_t \phi \circ z)(x_1,t) + \frac{1}{2} |\mathbf{v}(x_1,t)|^2 + (p \circ z)(x_1,t) + gz_2(x_1,t) = f(t),$$

so that

$$\partial_1(\partial_t\phi\circ z)=-\partial_1\left(\frac{1}{2}|\boldsymbol{v}|^2+(p\circ z)+gz_2\right),$$

where we have used the boundary condition (11c) in the last equality. Using (15), we find that

$$\partial_t \overline{\omega} = \partial_1 \left(\frac{1}{2} |\boldsymbol{v}|^2 + c \,\overline{\omega} + \lambda \frac{\partial_1^2 h}{(1 + (\partial_1 h)^2)^{3/2}} - g z_2 \right). \tag{16}$$

We now suppose that the interface $\Gamma(t)$ remains a graph and is given by (4). With the definition of the metric (7), we write the unit normal and tangent vectors, respectively, to $\Gamma(t)$ as

$$n = g^{-\frac{1}{2}}(-\partial_1 h, 1)$$
, and $\tau = g^{-\frac{1}{2}}(1, \partial_1 h)$.

Using (11e), we decompose \boldsymbol{v} as follows:

$$\mathbf{v} = (\mathbf{v} \cdot \mathbf{n})\mathbf{n} + (\mathbf{v} \cdot \boldsymbol{\tau})\boldsymbol{\tau} = g^{-\frac{1}{2}}\partial_t h \, \mathbf{n} + g^{-\frac{1}{2}}\bar{\omega} \, \boldsymbol{\tau} \,, \tag{17}$$

and hence

$$|\mathbf{v}|^2 = g^{-1}(|\partial_t h|^2 + |\bar{\omega}|^2).$$
 (18)

Equations (13) and (17) then provide us with the identity

$$c = \partial_t z_1 - \boldsymbol{v}_1 = -\boldsymbol{v}_1 = g^{-1} \left(\partial_t h \partial_1 h - \bar{\omega} \right),$$

so that (16) can be written as

$$\partial_t \bar{\omega} = -g \partial_1 h + \partial_1 \left[\frac{1}{2} g^{-1} (|\partial_t h|^2 + |\bar{\omega}|^2) - g^{-1} |\bar{\omega}|^2 + g^{-1} \bar{\omega} \partial_t h \partial_1 h \right] + \lambda \partial_1 \left(\frac{\partial_1^2 h}{(1 + (\partial_1 h)^2)^{3/2}} \right)$$

$$= -g \partial_1 h + \frac{1}{2} \partial_1 \left[g^{-1} \left(|\partial_t h|^2 - |\bar{\omega}|^2 + 2\bar{\omega} \partial_t h \partial_1 h \right) \right] + \lambda \partial_1 \left(\frac{\partial_1^2 h}{(1 + (\partial_1 h)^2)^{3/2}} \right). \tag{19}$$

3.3 The equation for the stream function

Since $\Omega(t)$ is simply connected, by classical Hodge theory, we can uniquely determine the velocity vector \boldsymbol{u} by solving the following elliptic system:

curl
$$\mathbf{u} = 0$$
 and div $\mathbf{u} = 0$ in $\Omega(t)$, and $\mathbf{u} \cdot \boldsymbol{\tau} = \omega$ on $\Gamma(t)$. (20)

Solutions of (20) have the form $\boldsymbol{u} = \nabla^{\perp} \vartheta$ for some stream function ϑ which satisfies the scalar Neumann problem

$$\Delta \vartheta = 0 \text{ in } \Omega(t), \text{ and } \frac{\partial \vartheta}{\partial \mathbf{M}} = -\omega \text{ on } \Gamma(t).$$
 (21)

Existence, uniqueness, and regularity of solutions to (21) is classical when $\Gamma(t)$ is sufficiently smooth and $\int_{\Gamma(t)} \omega dS(t) = 0$; see [23] for the case that $\Gamma(t)$ is of Sobolev class.

3.4 The evolution equation for the free-surface

We extend the parameterization (4) to a diffeomorphism ψ of \mathcal{D} as

$$\psi(x_1, x_2) = (x_1, x_2 + h(x_1, t)) \qquad \forall (x_1, x_2) \in \mathcal{D},$$
(22)

and set

$$\nabla \psi = \begin{bmatrix} 1 & 0 \\ \partial_1 h & 1 \end{bmatrix}, \quad A = (\nabla \psi)^{-1} = \begin{bmatrix} 1 & 0 \\ -\partial_1 h & 1 \end{bmatrix}. \tag{23}$$

We then define the stream function on the reference domain \mathcal{D} as $\varphi = \vartheta \circ \psi$. We then compute that

$$\boldsymbol{v} = \boldsymbol{u} \circ \psi = (\nabla^{\perp} \vartheta) \circ \psi = (-A_2^k \partial_k \varphi, A_1^k \partial_k \varphi) = (-\partial_2 \varphi, \partial_1 \varphi - \partial_1 h \partial_2 \varphi).$$

From (11e), $\partial_t h(x_1, t) = \boldsymbol{v} \cdot (-\partial_1 h, 1)$ on \mathbb{S}^1 , so that

$$\partial_t h = \partial_1 \varphi$$
 on \mathbb{S}^1 . (24)

4 Stokes expansion and linear recursion for the time-dependent water waves

4.1 Stokes expansion

Letting $0 < \epsilon < 1$ denote the steepness parameter (which can be viewed as the ratio of the amplitude to characteristic wavelength), we consider the following Stokes expansion ansatz:

$$h(x_1, t) = \epsilon \widetilde{h}(x_1, t), \quad \varphi(x, t) = \epsilon \widetilde{\varphi}(x, t), \quad \overline{\omega}(x_1, t) = \epsilon \widetilde{\omega}(x_1, t),$$
 (25)

where

$$\tilde{h}(x_1, t) = h_0(x_1, t) + \epsilon h_1(x_1, t) + \epsilon^2 h_2(x_1, t) + \cdots,$$
(26a)

$$\widetilde{\varphi}(x,t) = \varphi_0(x,t) + \epsilon \varphi_1(x,t) + \epsilon^2 \varphi_2(x,t) + \cdots,$$
 (26b)

$$\widetilde{\omega}(x_1, t) = \omega_0(x_1, t) + \epsilon \omega_1(x_1, t) + \epsilon^2 \omega_2(x_1, t) + \cdots$$
(26c)

In particular, at the initial time t = 0, we have

$$(h(x_1, 0), \partial_t h(x_1, 0)) = (h_{\text{init}}(x_1), \dot{h}_{\text{init}}(x_1)) \text{ for all } x_1 \in \mathbb{S}^1.$$
 (27)

or, equivalently,

$$(\widetilde{h}(x_1,0), \partial_t \widetilde{h}(x_1,0)) = \left(\frac{h_{\text{init}}(x_1)}{\epsilon}, \frac{\dot{h}_{\text{init}}(x_1)}{\epsilon}\right) \text{ for all } x_1 \in \mathbb{S}^1.$$
 (28)

4.2 Linear recursion for the stream function

Using (23), the scalar Neumann problem (21) can be written as

$$\partial_k (A_\ell^k A_\ell^j \partial_j \varphi) = 0 \quad \text{in} \quad \mathcal{D},$$
 (29a)

$$A_{\ell}^{k} \partial_{k} \varphi \mathbf{n}_{\ell} = -\omega \circ \psi \quad \text{on } \mathbb{S}^{1}.$$
 (29b)

and in expanded form,

$$\Delta \varphi = 2\partial_1 h \partial_{12} \varphi + \partial_1^2 h \partial_2 \varphi - (\partial_1 h)^2 \partial_2^2 \varphi \qquad \text{in } \mathcal{D}, \qquad (30a)$$

$$\frac{\partial \varphi}{\partial \mathbf{N}} = -\frac{\bar{\omega}}{1 + (\partial_1 h)^2} + \frac{\partial_1 h}{1 + (\partial_1 h)^2} \partial_1 \varphi \qquad \text{on } \mathbb{S}^1.$$
 (30b)

Substitution of our Stokes expansion (25) shows that (30) is equivalent to the following linear recursion relation for $k \ge 0$:

$$\Delta \varphi_k = \partial_2 \left[\sum_{j=0}^{k-1} \left(2 \partial_1 h_j \partial_1 \varphi_{k-1-j} + \partial_1^2 h_j \varphi_{k-1-j} \right) - \sum_{j=0}^{k-2} \sum_{r=0}^{j} \partial_1 h_r \partial_1 h_{j-r} \partial_2 \varphi_{k-2-j} \right] \text{ in } \mathcal{D},$$
(31a)

$$\frac{\partial \varphi_k}{\partial \mathbf{N}} = -\omega_k + \sum_{j=0}^{k-1} \partial_1 h_j \partial_1 \varphi_{k-1-j} - \sum_{j=0}^{k-2} \sum_{r=0}^j \partial_1 h_r \partial_1 h_{j-r} \partial_2 \varphi_{k-2-j}$$
 on \mathbb{S}^1 . (31b)

4.3 Linear recursion for the height function

Substitution of (25) into (24) shows that

$$\partial_t h_k = \partial_1 \varphi_k \quad \text{on } \mathbb{S}^1.$$
 (32)

4.4 Linear recursion for the tangential velocity

In absence of surface tension effects ($\lambda = 0$), we have that (19) is equivalent to

$$\partial_t \bar{\omega} = -g \partial_1 h + \frac{1}{2} \partial_1 \left[(1 + (\partial_1 h)^2)^{-1} \left(|\partial_t h|^2 - |\bar{\omega}|^2 + 2\bar{\omega}\partial_t h \partial_1 h \right) \right]$$

$$= -g \partial_1 h + (1 + (\partial_1 h)^2) \frac{\partial_1 \left[|\partial_t h|^2 - |\bar{\omega}|^2 + 2\bar{\omega}\partial_t h \partial_1 h \right]}{2}$$

$$- \partial_1 h \partial_1^2 h \left[|\partial_t h|^2 - |\bar{\omega}|^2 + 2\bar{\omega}\partial_t h \partial_1 h \right] - \partial_t \bar{\omega} (2(\partial_1 h)^2 + (\partial_1 h)^4)$$

$$- g \partial_1 h (2(\partial_1 h)^2 + (\partial_1 h)^4). \tag{33}$$

Substitution of the asymptotic expansion (26) into (19) shows that

$$\partial_{t}\omega_{k} = -g\partial_{1}h_{k} + \sum_{\ell=0}^{k-1} \frac{\partial_{1} \left[\partial_{t}h_{k-1-\ell}\partial_{t}h_{\ell} - \omega_{\ell}\omega_{k-1-\ell}\right]}{2} + \sum_{\ell=0}^{k-2} \sum_{n=0}^{\ell} \partial_{1} \left[\omega_{n}\partial_{t}h_{\ell-n}\partial_{1}h_{k-2-\ell}\right] \\
+ \sum_{\ell=0}^{k-3} \sum_{n=0}^{\ell} \sum_{j=0}^{n} \partial_{1}h_{j}\partial_{1}h_{n-j} \frac{\partial_{1} \left[\partial_{t}h_{\ell-n}\partial_{t}h_{k-3-\ell} - \omega_{\ell-n}\omega_{k-3-\ell}\right]}{2} \\
+ \sum_{\ell=0}^{k-4} \sum_{n=0}^{\ell} \sum_{j=0}^{n} \sum_{m=0}^{j} \partial_{1}h_{m}\partial_{1}h_{j-m}\partial_{1} \left[\omega_{n-j}\partial_{t}h_{\ell-n}\partial_{1}h_{k-4-\ell}\right] \\
- \sum_{\ell=0}^{k-3} \sum_{n=0}^{\ell} \sum_{j=0}^{n} \partial_{1}h_{j}\partial_{1}^{2}h_{n-j} \left[\partial_{t}h_{\ell-n}\partial_{t}h_{k-\ell} - \omega_{\ell-n}\omega_{k-3-\ell}\right] \\
- 2\sum_{\ell=0}^{k-4} \sum_{n=0}^{\ell} \sum_{j=0}^{n} \sum_{m=0}^{j} \partial_{1}h_{m}\partial_{1}^{2}h_{j-m}\omega_{n-j}\partial_{t}h_{\ell-n}\partial_{1}h_{k-4-\ell} \\
- 2\sum_{\ell=0}^{k-2} \sum_{n=0}^{\ell} \partial_{t}\omega_{n}\partial_{1}h_{\ell-n}\partial_{1}h_{k-2-\ell} - 2g\sum_{\ell=0}^{k-2} \sum_{n=0}^{\ell} \partial_{1}h_{n}\partial_{1}h_{\ell-n}\partial_{1}h_{k-2-\ell} \\
- \sum_{\ell=0}^{k-4} \sum_{n=0}^{\ell} \sum_{j=0}^{n} \sum_{m=0}^{j} \partial_{t}\omega_{m}\partial_{1}h_{j-m}\partial_{1}h_{n-j}\partial_{1}h_{\ell-n}\partial_{1}h_{k-4-\ell} \\
- g\sum_{\ell=0}^{k-4} \sum_{n=0}^{\ell} \sum_{j=0}^{n} \sum_{m=0}^{j} \partial_{1}h_{m}\partial_{1}h_{j-m}\partial_{1}h_{n-j}\partial_{1}h_{\ell-n}\partial_{1}h_{k-4-\ell} . \tag{34}$$

5 Derivation of the quadratic and cubic h-models

5.1 Preliminary lemmas

The linear recursion for the stream function φ_k given in (31) can be decomposed into simpler elliptic equations. Thus, given certain forcing functions h, φ and g, we shall focus on the following two elliptic equations

$$\Delta X = \partial_2 \left[2(\partial_1 h)(\partial_1 \varphi) + (\partial_1^2 h) \varphi \right] \text{ in } \mathcal{D}, \text{ and } \partial_2 X = (\partial_1 h)(\partial_1 \varphi) \text{ on } \mathbb{S}^1,$$
 (35)

and

$$\Delta Y = \partial_2 g \text{ in } D, \text{ and } \partial_2 Y = g \text{ on } \mathbb{S}^1.$$
 (36)

We shall make use of two lemmas that show that the restriction of the solutions of (35) and (35) to \mathbb{S}^1 can be expressed in terms of the functions on \mathbb{S}^1 : h_0, \dots, h_{k-1} and $\omega_0, \dots, \omega_{k-1}$.

Following our discussion in Section 2.6, a harmonic function $f(x_1, x_2)$ in \mathcal{D} can be expanded as

$$f(x_1, x_2) = \sum_{n = -\infty}^{\infty} \widehat{f}(n)e^{inx_1 + |n|x_2} \quad \text{for all } (x_1, x_2) \in \mathcal{D}$$

for some complex coefficients $\widehat{f}(n)$ that do not depend on x_2 . For example, the stream function φ_0 , solving (31) with k=0, is harmonic and hence $\varphi_0(x_1,x_2) = \sum_{n\in\mathbb{Z}} \widehat{\varphi_0}(n)e^{inx_1+|n|x_2}$.

For k = 1, the right-hand side of (31a) is given by

$$\partial_2 \left[2(\partial_1 h_0)(\partial_1 \varphi_0) + (\partial_1^2 h_0) \varphi_0 \right](x_1, x_2) = \sum_{n = -\infty}^{\infty} \sum_{m = -\infty}^{\infty} |m|(m^2 - n^2) \widehat{h_0}(n - m) \widehat{\varphi_0}(m) e^{inx_1 + |m|x_2},$$

and the right-hand side of (31b) is

$$(\partial_1 h_0)(\partial_1 \varphi_0) = -\sum_{n=-\infty}^{\infty} \sum_{m=-\infty}^{\infty} m(n-m)\widehat{h_0}(n-m)\widehat{\varphi_0}(m)e^{inx_1+|m|x_2}.$$

It follows that the solution φ_1 can be written via the expansion

$$\varphi_1(x_1, x_2) = \sum_{n, m \in \mathbb{Z}} \widehat{P}_{1n, m} e^{inx_1 + |m|x_2},$$

where $\sum_{n,m\in\mathbb{Z}}$ denotes the double sum $\sum_{n=-\infty}^{\infty}\sum_{m=-\infty}^{\infty}$ and $\{\widehat{P}_{1n,m}\}_{n,m\in\mathbb{Z}}$ is a (double) sequence of complex numbers. Using the recursion formula (31), an induction argument then shows that for all $j\in\mathbb{N}$, the stream function φ_j can be written as the expansion

$$\varphi_j(x_1, x_2) = \sum_{n, m \in \mathbb{Z}} \widehat{P}_{j_{n,m}}(x_2) e^{inx_1 + |m|x_2},$$

where for each fixed j, n, m, $\widehat{P}_{j_{n,m}}(x_2)$ is a polynomial (of degree j-1) function of x_2 . This motivates the following two lemmas.

Lemma 1. Let $h: \mathbb{S}^1 \to \mathbb{R}$ and $\varphi: \mathcal{D} \to \mathbb{R}$ denote 2π -periodic functions of x_1 , such that $h(x_1) = \sum_{k \in \mathbb{Z}, k \neq 0} \hat{h}_k e^{ikx_1}, \quad \varphi(x_1, x_2) = \sum_{k, m \in \mathbb{Z}} \hat{P}_{k,m}(x_2) e^{ikx_1 + |m|x_2},$

where $x_2 \mapsto \hat{P}_{k,m}(x_2)$ is a polynomial function. If X is the unique solution to (35), then

$$(\partial_1 X)(x_1, 0) = -H[(\partial_1 h)(\partial_1 \varphi)] - \sum_{k, \ell, m \in \mathbb{Z}} i \operatorname{sgn}(k) |m| (\ell^2 - k^2) \hat{h}_{k-\ell} \sum_{j=0}^{\infty} \frac{(-1)^j \hat{P}_{\ell, m}^{(j)}(0)}{(|m| + |k|)^{j+1}} e^{ikx_1},$$
(37)

where $\hat{P}_{\ell,m}^{(j)}(0)$ denotes $\hat{\sigma}_2^j \hat{P}_{\ell,m}(x_2)$ evaluated at $x_2 = 0$. Moreover, if φ is harmonic in \mathcal{D} so that $\varphi(x_1, x_2) = \sum_{k \in \mathbb{Z}} \hat{\varphi}_k e^{ikx_1 + |k|x_2}$, then

$$\partial_1 X = -\Lambda [h \partial_1 \varphi] + \partial_1 (h \Lambda \varphi) = \partial_1 (\llbracket h, H \rrbracket \partial_1 \varphi) \quad on \quad \mathbb{S}^1, \tag{38}$$

where $[\cdot,\cdot]$ denotes the commutator.

Proof. With $X(x_1, x_2) = \sum_{k \in \mathbb{Z}} \hat{X}_k(x_2) e^{ikx_1}$, $\hat{X}_k(x_2)$ satisfies the differential equation

$$\hat{\sigma}_{2}^{2} \hat{X}_{k}(x_{2}) - k^{2} \hat{X}_{k}(x_{2}) = \sum_{\ell, m \in \mathbb{Z}} |m| (\ell^{2} - k^{2}) \hat{h}_{k-\ell} \hat{P}_{\ell, m} e^{|m|x_{2}} \quad \text{for } x_{2} < 0 \,,$$

$$(\hat{\sigma}_{2} \hat{X}_{k})(0) = \sum_{\ell, m \in \mathbb{Z}} (\ell - k) \ell \hat{h}_{k-\ell} \hat{P}_{\ell, m} \,,$$

whose solution is given by the variation-of-parameters formula: for $k \neq 0$,

$$\begin{split} \hat{X}_k(x_2) &= \frac{1}{|k|} \sum_{\ell,m \in \mathbb{Z}} (\ell - k) \ell \hat{h}_{k-\ell} \hat{P}_{\ell,m}(0) e^{|k|x_2} \\ &- \sum_{\ell,m \in \mathbb{Z}} \frac{|m|(\ell^2 - k^2)}{2|k|} \hat{h}_{k-\ell} \left(e^{|k|x_2} + e^{-|k|x_2} \right) \sum_{j=0}^{\infty} \frac{(-1)^j \hat{P}_{\ell,m}^{(j)}(0)}{(|m| + |k|)^{j+1}} \\ &+ \sum_{\ell m \in \mathbb{Z}} \frac{|m|(\ell^2 - k^2)}{2k} \hat{h}_{k-\ell} \int_0^{x_2} \hat{P}_{\ell,m}(y_2) \left[e^{(|m| - k)y_2 + kx_2} - e^{(|m| + k)y_2 - kx_2} \right] dy_2 \,. \end{split}$$

Therefore,

$$ik\hat{X}_{k}(0) = i\operatorname{sgn}(k) \sum_{\ell,m \in \mathbb{Z}} \left[(\ell - k)\ell \hat{h}_{k-\ell} \hat{P}_{\ell,m} - |m|(\ell^{2} - k^{2}) \hat{h}_{k-\ell} \sum_{j=0}^{\infty} \frac{(-1)^{j} \hat{P}_{\ell,m}^{(j)}(0)}{(|m| + |k|)^{j+1}} \right], \quad (39)$$

and (37) follows from the Fourier inversion formula.

In the case that φ is harmonic in \mathcal{D} or equivalently, the Fourier coefficients are given as $\hat{P}_{\ell,m} = \hat{\varphi}_{\ell}$ if $\ell = m$ and $\hat{P}_{\ell,m} = 0$ if $\ell \neq m$, then the identity (39) shows that

$$ik\widehat{X}_{k}(0) = i\operatorname{sgn}(k) \sum_{\ell \in \mathbb{Z}} (\ell - k)\ell \widehat{h}_{k-\ell} \sum_{m \in \mathbb{Z}} \widehat{P}_{\ell,m} - i\operatorname{sgn}(k) \sum_{\ell \in \mathbb{Z}} \frac{|m|(\ell^{2} - k^{2})}{|m| + |k|} \widehat{h}_{k-\ell} \sum_{m \in \mathbb{Z}} \widehat{P}_{\ell m}$$

$$= i\operatorname{sgn}(k) \sum_{\ell \in \mathbb{Z}} (\ell - k)\ell \widehat{h}_{k-\ell} \widehat{\varphi}_{\ell} - i\operatorname{sgn}(k) \sum_{\ell \in \mathbb{Z}} \frac{|\ell|(\ell^{2} - k^{2})}{|\ell| + |k|} \widehat{h}_{k-\ell} \widehat{\varphi}_{\ell}$$

$$= i\operatorname{sgn}(k) \sum_{\ell \in \mathbb{Z}} \left[i(k - \ell) \widehat{h}_{k-\ell} \right] (i\ell \widehat{\varphi}_{\ell}) - i\operatorname{sgn}(k) \sum_{\ell \in \mathbb{Z}} (|\ell| - |k|) \widehat{h}_{k-\ell} \widehat{\Lambda} \widehat{\varphi}_{\ell}$$

and hence on \mathbb{S}^1 ,

$$\begin{split} \partial_1 X &= -H \big[(\partial_1 h)(\partial_1 \varphi) \big] + H(h\Lambda \varphi) + \partial_1 (h\Lambda \varphi) \\ &= -H \big[h\partial_1^2 \varphi + (\partial_1 h)(\partial_1 \varphi) \big] + \partial_1 (h\Lambda \varphi) = -\Lambda (h\partial_1 \varphi) + \partial_1 (h\Lambda \varphi) \end{split}$$

from which (38) follows.

Lemma 2. Let $g: \mathcal{D} \to \mathbb{R}$ be a 2π -periodic function of x_1 , such that

$$g(x_1, x_2) = \sum_{k,m \in \mathbb{Z}} \widehat{g}_{k,m} e^{ikx_1 + |m|x_2},$$

and let Y denote the unique solution to (36). Then

$$\partial_1 Y = -Hg - i\operatorname{sgn}(k) \sum_{k, m \in \mathbb{Z}} \frac{|m|}{|m| + |k|} \widehat{g}_{k,m} e^{ikx_1} \quad on \quad \mathbb{S}^1.$$
 (40)

Proof. Letting $Y(x_1, x_2) = \sum_{k \in \mathbb{Z}} \hat{Y}_k(x_2) e^{ikx_1}$, we find that

$$\partial_2^2 \widehat{Y}_k(x_2) - k^2 \widehat{Y}_k(x_2) = \sum_{m \in \mathbb{Z}} |m| \widehat{g}_{k,m} e^{|m|x_2} \quad \text{for } x_2 < 0,$$

$$\partial_2 \widehat{Y}_k(0) = \sum_{m \in \mathbb{Z}} \widehat{g}_{k,m}.$$

The solution for the case $k \neq 0$ is obtained via the variation-of-parameters formula as

$$\begin{split} \widehat{Y}_k(x_2) &= \frac{1}{|k|} \sum_{m \in \mathbb{Z}} \widehat{g}_{k,m} e^{|k|x_2} - \frac{1}{2|k|} \sum_{m \in \mathbb{Z}} \frac{|m|}{|m| + |k|} \widehat{g}_{k,m} (e^{|k|x_2} + e^{-|k|x_2}) \\ &+ \sum_{m \in \mathbb{Z}} \frac{|m|}{2k} \widehat{g}_{k,m} \int_0^{x_2} \left[e^{(|m| - k)x_2 + kx_2} - e^{(|m| + k)x_2 - kx_2} \right] dx_2 \,. \end{split}$$

Therefore,

$$ik\hat{Y}_k(0) = i\operatorname{sgn}(k) \sum_{m \in \mathbb{Z}} \hat{g}_{k,m} - i\operatorname{sgn}(k) \sum_{m \in \mathbb{Z}} \frac{|m|}{|m| + |k|} \hat{g}_{k,m}$$

which is (40).

5.2 The quadratic h-model

From (31),

$$\Delta \varphi_0 = 0 \text{ in } \mathcal{D} \text{ and } \frac{\partial \varphi_0}{\partial \mathbf{N}} = -\omega_0 \text{ on } \mathbb{S}^1,$$
 (41)

and

$$\Delta \varphi_1 = \partial_2 \left(2 \partial_1 h_0 \partial_1 \varphi_0 + \partial_1^2 h_0 \varphi_0 \right) \text{ in } \mathcal{D} \text{ and } \frac{\partial \varphi_1}{\partial \mathbf{N}} = -\omega_1 + \partial_1 h_0 \partial_1 \varphi_0 \text{ on } \mathbb{S}^1.$$
 (42)

We decompose $\varphi_1 = \varphi_1^{(a)} + \varphi_1^{(b)}$, where $\varphi_1^{(a)}$ and $\varphi_1^{(b)}$ satisfy

$$\Delta \varphi_1^{(a)} = f := \partial_2 \left(2 \partial_1 h_0 \partial_1 \varphi_0 + \partial_1^2 h_0 \varphi_0 \right) \quad \text{in } \mathcal{D}, \tag{43a}$$

$$\frac{\partial \varphi_1^{(a)}}{\partial \mathbf{N}} = \mathbf{g} := \partial_1 h_0 \partial_1 \varphi_0 \qquad \text{on } \mathbb{S}^1, \tag{43b}$$

and

$$\Delta \varphi_1^{(b)} = 0 \quad \text{in } \mathcal{D},$$
 (44a)

$$\frac{\partial \varphi_1^{(b)}}{\partial \mathbf{N}} = -\omega_1 \quad \text{on } \mathbb{S}^1. \tag{44b}$$

We note that the solvability condition for (43) is satisfied since integration-by-parts shows that

$$\int_{\mathbb{S}^1\times\mathbb{R}^-} \partial_2 \left(2\partial_1 h_0 \partial_1 \varphi_0 + \partial_1^2 h_0 \ \varphi_0\right) dy = \int_{\mathbb{S}^1} 2\partial_1 h_0 \partial_1 \varphi_0 + \partial_1^2 h_0 \ \varphi_0 dx_1 = \int_{\mathbb{S}^1} \partial_1 h_0 \partial_1 \varphi_0 dx_1 \,,$$

and similarly the solvability condition for (44) is also satisfied: $\int_{\mathbb{S}^1} \omega_1 dx_1 = 0$. With the solvability conditions satisfied, the elliptic problems (43) and (44) have unique solutions in $H^1(\mathcal{D})$ by the Lax-Milgram theorem. Using the Hilbert transform,

$$\partial_1 \varphi_0 = H\omega_0 \text{ and } \partial_1 \varphi_1^{(b)} = H\omega_1 \text{ on } \mathbb{S}^1.$$
 (45)

We can then apply Lemma 1 and conclude that

$$\partial_1 \varphi_1^{(a)}(x_1, 0, t) = \partial_1 (\llbracket h_0, H \rrbracket H \omega_0) = -H [(\partial_1 h_0)(H \omega_0) + h_0 \Lambda \omega_0] - \partial_1 (h_0 \omega_0) \quad \text{on } \mathbb{S}^1.$$
 (46)

From the recursion for the tangential velocity and (32), we have that

$$\partial_t h_0 = H\omega_0$$
 on \mathbb{S}^1 , (47a)

$$\partial_t \omega_0 = -g \partial_1 h_0$$
 on \mathbb{S}^1 , (47b)

$$\partial_t h_1 = H\omega_1 - H[(\partial_1 h_0)(H\omega_0) + h_0 \Lambda \omega_0] - \partial_1 (h_0 \omega_0) \text{ on } \mathbb{S}^1,$$
(47c)

$$\partial_t \omega_1 = -g \partial_1 h_1 + \frac{1}{2} \partial_1 \left(|\partial_t h_0|^2 - |\omega_0|^2 \right) \qquad \text{on } \mathbb{S}^1.$$
 (47d)

We can write (47) as system of wave equations,

$$\partial_t^2 h_0 + g\Lambda h_0 = 0$$

$$\partial_t^2 h_1 + g\Lambda h_1 = \frac{1}{2} \Lambda \left(|\partial_t h_0|^2 - |H\partial_t h_0|^2 \right)$$

$$- H \left[(\partial_1 \partial_t h_0)(\partial_t h_0) - g(\partial_1 h_0)(\Lambda h_0) + (\partial_t h_0)(\partial_1 \partial_t h_0) - gh_0 \Lambda \partial_1 h_0 \right]$$

$$+ \partial_1 \left[(\partial_t h_0)(H\partial_t h_0) \right] + g\partial_1 (h_0 \partial_1 h_0)$$

$$= -\Lambda (|H\partial_t h_0|^2) + g\Lambda (h_0 \Lambda h_0) + g\partial_1 (h_0 \partial_1 h_0) ,$$

$$(48b)$$

where, in the last equality, we have used the Tricomi identity

$$2H(fHf) = (Hf)^2 - f^2. (49)$$

The quadratic h-model follows from setting

$$h(x_1, t) = \epsilon h_0(x_1, t) + \epsilon^2 h_1(x_1, t), \qquad (50)$$

so that

$$\partial_t^2 h + g\Lambda h = \epsilon^2 \left(-\Lambda(|H\partial_t h_0|^2) + g\Lambda(h_0\Lambda h_0) + g\partial_1(h_0\partial_1 h_0) \right)$$

= $-\Lambda(|H\partial_t h|^2) + g\Lambda(h\Lambda h) + g\partial_1(h\partial_1 h) + \mathcal{O}(\epsilon^3)$.

Neglecting terms of order $O(\epsilon^3)$, the quadratic h-model reads

$$\partial_t^2 h + g\Lambda h = -\Lambda(|H\partial_t h|^2) - g\partial_1(\llbracket h, H \rrbracket \Lambda h), \qquad (51a)$$

$$= 2\partial_1(\partial_t h H \partial_t h) - \Lambda\left((\partial_t h)^2\right) + g\Lambda(h\Lambda h) + g\partial_1(h\partial_1 h). \tag{51b}$$

The quadratic h-model (51) modeling gravity water waves in deep water reduces to the "Model" equation obtained by Akers & Milewski [2], although in a very different way. They first simplify the water waves problem by making the assumption that the potential function at each recursion relation is set on the fixed domain with top boundary given by $x_2 = 0$ (rather than $x_2 = h(x_1, t)$). It is interesting to note that up to quadratic nonlinearity, this simplification produces the same h-model as we have obtained by keeping the full water waves system in the asymptotics. We note that Akers & Nicholls [3] later used a diffeomorphism (similar to our ϕ) to fix the domain, but only study the linear recursion for the traveling solitary wave ansatz.

Remark 1. We observe that the quadratic h-model (51) is kept invariant by the scaling

$$h_{\mu}(x_1, t) = \frac{1}{\mu^2} h(\mu^2 x_1, \mu t).$$

This is the same scale invariance as for the full gravity water wave problem.

Remark 2. Following a similar approach, for the case of an internal wave separating two perfect fluids with densities ρ^+ and ρ^- , we can derive the equation

$$\partial_t^2 h = Ag\Lambda h + A\Lambda(|H\partial_t h|^2) + A^2 g\left(\Lambda(h\Lambda h) + \partial_1(h\partial_1 h)\right)$$
(52)

where

$$A = \frac{\rho^+ - \rho^-}{\rho^+ + \rho^-}$$

is the Atwood number.

A similar asymptotic model was derived in Granero-Belinchón & Shkoller [38] to study the two-fluid problem.

5.3 The quadratic h-model with surface tension

For surface waves in the regime where the effects of both gravity and surface tension are similar in magnitude (wavelengths of order $L \approx \sqrt{73.5/981}cm$ or, equivalently, the Bond number $\frac{\lambda}{gL^2} \approx 1$), the previous recursion for the tangential velocity has to be changed. This is somewhat challenging for general k due to the denominator present in the expression for the mean curvature; however, for k=0 and 1 this modification takes the following form:

$$\partial_t h_0 = H\omega_0 \qquad \qquad \text{on } \mathbb{S}^1, \qquad (53a)$$

$$\partial_t \omega_0 = -g \partial_1 h_0 + \lambda \partial_1^3 h_0 \qquad \text{on } \mathbb{S}^1, \qquad (53b)$$

$$\partial_t h_1 = H\omega_1 - H[(\partial_1 h_0)(H\omega_0) + h_0 \Lambda \omega_0] - \partial_1 (h_0 \omega_0) \text{ on } \mathbb{S}^1,$$
 (53c)

$$\partial_t \omega_1 = -g \partial_1 h_1 + \lambda \partial_1^3 h_1 + \frac{1}{2} \partial_1 \left(|\partial_t h_0|^2 - |\omega_0|^2 \right) \quad \text{on} \quad \mathbb{S}^1.$$
 (53d)

Equivalently, taking a time derivative, we have that

$$\partial_t^2 h_0 = -g\Lambda h_0 - \lambda \Lambda^3 h_0$$

$$\begin{split} \partial_t^2 h_1 &= -g\Lambda h_1 - \lambda \Lambda^3 h_1 + \frac{1}{2}\Lambda \left(|\partial_t h_0|^2 - |H\partial_t h_0|^2 \right) \\ &- H \Big[(\partial_1 \partial_t h_0)(\partial_t h_0) + (\partial_1 h_0)(H\partial_t \omega_0) + \partial_t h_0 \partial_1 \partial_t h_0 + h_0 \Lambda \partial_t \omega_0 \Big] \\ &- \partial_1 (\partial_t h_0 \omega_0 + h_0 \partial_t \omega_0) \\ &= -g\Lambda h_1 - \lambda \Lambda^3 h_1 - \Lambda \left(|H\partial_t h_0|^2 \right) - \Lambda \Big[h_0 H\partial_t \omega_0 \Big] - \partial_1 (h_0 \partial_t \omega_0) \\ &= -g\Lambda h_1 - \lambda \Lambda^3 h_1 - \Lambda \left(|H\partial_t h_0|^2 \right) + \Lambda \Big[h_0 \left(g\Lambda h_0 + \lambda \Lambda^3 h_0 \right) \Big] - \partial_1 \left(h_0 \left(-g\partial_1 h_0 + \lambda \partial_1^3 h_0 \right) \right) \,. \end{split}$$

Then, a similar argument as before shows that, up to $\mathcal{O}(\epsilon^3)$, the quadratic h-model (51) with surface tension modeling gravity-capillary waves in deep water is written as

$$\partial_t^2 h = -g\Lambda h - \lambda \Lambda^3 h - \Lambda (|H\partial_t h|^2) + \Lambda [h (g\Lambda h + \lambda \Lambda^3 h)] - \partial_1 (h (-g\partial_1 h + \lambda \partial_1^3 h)).$$
 (54)

5.4 The cubic h-model

In order to derive the cubic h-model, we shall also need the equation that φ_2 satisfies; thus, in addition to (41) and (42), we use (31) to find that

$$\Delta \varphi_2 = \partial_2 \left[2\partial_1 h_0 \partial_{12} \varphi_1 + 2\partial_1 h_1 \partial_1 \varphi_0 + \varphi_1 \partial_1^2 h_0 + \varphi_0 \partial_1^2 h_1 - (\partial_1 h_0)^2 \partial_2 \varphi_0 \right] \quad \text{in } \mathcal{D}, \quad (55a)$$

$$\frac{\partial \varphi_2}{\partial \mathbf{N}} = -\omega_2 + \partial_1 h_0 \partial_1 \varphi_1 + \partial_1 h_1 \partial_1 \varphi_0 - (\partial_1 h_0)^2 \partial_2 \varphi_0 \qquad \text{on } \mathbb{S}^1. \tag{55b}$$

We decompose φ_2 as the sum $\varphi_2 = \varphi_2^{(a)} + \varphi_2^{(b)} + \varphi_2^{(c)} + \varphi_2^{(d)}$, where $\varphi_2^{(a)}$, $\varphi_2^{(b)}$, $\varphi_2^{(c)}$ and $\varphi_2^{(d)}$ satisfy

$$\Delta \varphi_{2}^{(a)} = 2\partial_{1}h_{1}\partial_{12}\varphi_{0} + \partial_{1}^{2}h_{1}\partial_{2}\varphi_{0} \text{ in } \mathcal{D} \qquad \frac{\partial \varphi_{2}^{(a)}}{\partial \mathbf{N}} = \partial_{1}h_{1}\partial_{1}\varphi_{0} \text{ on } \mathbb{S}^{1},$$

$$\Delta \varphi_{2}^{(b)} = 2\partial_{1}h_{0}\partial_{12}\varphi_{1} + \partial_{1}^{2}h_{0}\partial_{2}\varphi_{1} \text{ in } \mathcal{D} \qquad \frac{\partial \varphi_{2}^{(b)}}{\partial \mathbf{N}} = \partial_{1}h_{0}\partial_{1}\varphi_{1} \text{ on } \mathbb{S}^{1},$$

$$\Delta \varphi_{2}^{(c)} = -(\partial_{1}h_{0})^{2}\partial_{2}^{2}\varphi_{0} \text{ in } \mathcal{D} \qquad \frac{\partial \varphi_{2}^{(c)}}{\partial \mathbf{N}} = -(\partial_{1}h_{0})^{2}\partial_{2}\varphi_{0} \text{ on } \mathbb{S}^{1},$$

$$\Delta \varphi_{2}^{(d)} = 0 \text{ in } \mathcal{D} \qquad \frac{\partial \varphi_{2}^{(c)}}{\partial \mathbf{N}} = -\omega_{2} \text{ on } \mathbb{S}^{1}.$$

Note that $\partial_1 \varphi_2^{(d)} = H\omega_2$ on \mathbb{S}^1 .

Solving (41),
$$\varphi_0(x_1, x_2, t) = -\sum_{k \in \mathbb{Z}, k \neq 0} \frac{\widehat{\omega_{0k}(t)}}{|k|} e^{ikx_1 + |k|x_2}$$
, and by Lemma 1,

$$\widehat{\sigma}_1 \varphi_2^{(a)} = \widehat{\sigma}_1(\llbracket h_1, H \rrbracket H \omega_0). \tag{56}$$

Next, we write the solution to (44) using the Fourier components $\widehat{\varphi_1^{(b)}}(k, x_2, t) = -\frac{\widehat{\omega_1}_k(t)}{|k|}e^{|k|x_2}$, and using the variation-of-parameters solution to (43), we see that

$$\begin{split} \widehat{\varphi_1^{(\mathrm{a})}}(k,x_2,t) &= \frac{\mathrm{sgn}(k)}{k} \widehat{\mathrm{g}}(k,t) e^{|k|x_2} + \int_0^{x_2} \widehat{\mathrm{f}}(k,y_2,t) \frac{e^{k(x_2-y_2)} - e^{k(y_2-x_2)}}{2k} dy_2 \\ &= \frac{(\widehat{\sigma_1(h_0H\omega_0)})_k(t)}{|k|} e^{|k|x_2} - \sum_{\ell \in \mathbb{Z}} \widehat{h_0}_{k-\ell}(t) \widehat{\omega_0}_\ell(t) e^{|\ell|x_2} \,; \end{split}$$

thus,

$$\varphi_1(x_1, x_2, t) = \sum_{k \in \mathbb{Z}} \frac{-\widehat{\omega_1}_k(t) + (\widehat{\partial_1}(\widehat{h_0}H\omega_0))_k(t)}{|k|} e^{ikx_1 + |k|x_2} - \sum_{k, \ell \in \mathbb{Z}} \widehat{h_0}_{k-\ell}(t) \widehat{\omega_0}_\ell(t) e^{ikx_1 + |\ell|x_2}.$$

It then follows from Lemma 1 with $\widehat{P}_{k,m} = \delta_{km} \frac{-\widehat{\omega}_{1k}(t) + (\widehat{\sigma}_{1}(\widehat{h}_{0}H\widehat{\omega}_{0}))_{k}(t)}{|k|} - \widehat{h}_{0k-m}(t)\widehat{\omega}_{0m}(t)$ that

$$\partial_{1}\varphi_{2}^{(b)} = \partial_{1}\left(\llbracket h_{0}, H \rrbracket H \omega_{1}\right) - \partial_{1}\left(\llbracket h_{0}, H \rrbracket \Lambda(h_{0}H\omega_{0})\right) + H\left[\left(\partial_{1}h_{0}\right)\partial_{1}(h_{0}\omega_{0})\right]
+ \sum_{k,\ell,m\in\mathbb{Z}} i\operatorname{sgn}(k) \frac{|m|(\ell^{2}-k^{2})}{|m|+|k|} \widehat{h_{0}}_{k-\ell} \widehat{h_{0}}_{\ell-m} \widehat{\omega_{0}}_{m} e^{ikx_{1}}
= \partial_{1}\left(\llbracket h_{0}, H \rrbracket H \omega_{1}\right) - \partial_{1}\left(\llbracket h_{0}, H \rrbracket \Lambda(h_{0}H\omega_{0})\right) + H\left[\left(\partial_{1}h_{0}\right)\partial_{1}(h_{0}\omega_{0})\right]
- \sum_{k,\ell,m\in\mathbb{Z}} \operatorname{sgn}(k) \frac{|m|(\ell+k)}{|m|+|k|} \widehat{\left(\partial_{1}h_{0}\right)}_{k-\ell} \widehat{h_{0}}_{\ell-m} \widehat{\omega_{0}}_{m} e^{ikx_{1}}.$$
(57)

Using Lemma 2 with $g = -(\partial_1 h_0)^2 (\partial_1 \varphi_0)$ (or equivalently with $\widehat{g}_{k,m} = (\widehat{\partial_1 h_0})^2_{k-m} \widehat{\omega}_{0m}$), we find that

$$(\partial_{1}\varphi_{2}^{(c)})(x_{1},0,t)$$

$$= -H\left[(\partial_{1}h_{0})^{2}\omega_{0}\right](t) - \sum_{k,\ell\in\mathbb{Z},k,\ell\neq0} i\operatorname{sgn}(k) \frac{|m|}{|m|+|k|} (\widehat{\partial_{1}h_{0}})^{2}_{k-m}(t)\widehat{\omega_{0}}_{m}(t)e^{ikx_{1}}$$

$$= -H\left[(\partial_{1}h_{0})^{2}\omega_{0}\right](t) - \sum_{k,\ell,m\in\mathbb{Z}} i\operatorname{sgn}(k) \frac{|m|}{|m|+|k|} (\widehat{\partial_{1}h_{0}})_{k-\ell}(t) (\widehat{\partial_{1}h_{0}})_{\ell-m}(t)\widehat{\omega_{0}}_{m}(t)e^{ikx_{1}}$$

$$= -H\left[(\partial_{1}h_{0})^{2}\omega_{0}\right](t) + \sum_{k,\ell,m\in\mathbb{Z}} \operatorname{sgn}(k) \frac{|m|(\ell-m)}{|m|+|k|} (\widehat{\partial_{1}h_{0}})_{k-\ell}(t) \widehat{h_{0}\ell-m}(t)\widehat{\omega_{0}}_{m}(t)e^{ikx_{1}}.$$
 (58)

Hence, combining (56), (57) and (58) and the fact that $\partial_1 \varphi_2^{(d)} = H\omega_2$ on \mathbb{S}^1 ,

$$\begin{split} &(\partial_1 \varphi_2)(x_1,0) = H\omega_2 + \partial_1(\llbracket h_1, H \rrbracket H\omega_0) + \partial_1\big(\llbracket h_0, H \rrbracket H\omega_1\big) - \partial_1\big(\llbracket h_0, H \rrbracket \Lambda(h_0 H\omega_0)\big) \\ &+ H\big[(\partial_1 h_0)\partial_1(h_0 \omega_0)\big] - H\big[(\partial_1 h_0)^2 \omega_0\big] - \sum_{k,\ell,m \in \mathbb{Z}} \operatorname{sgn}(k) \frac{|m|(m+k)}{|m|+|k|} \widehat{(\partial_1 h_0)}_{k-\ell} \widehat{h_0}_{\ell-m} \widehat{\omega_0}_m e^{ikx_1}. \end{split}$$

Noting that for each fixed $k, m \in \mathbb{Z}$,

$$\sum_{\ell\in\mathbb{Z}}\widehat{\partial_1 h_0}_{k-\ell}\widehat{h_0}_{\ell-m}=\widehat{h_0}\widehat{\partial_1 h_0}_{k-m}=\frac{1}{2}\widehat{\partial_1(h_0^2)}_{k-m}=\frac{i(k-m)}{2}\widehat{(h_0^2)}_{k-m}\,,$$

we have that

$$\begin{split} \sum_{k,\ell,m\in\mathbb{Z}} \operatorname{sgn}(k) \frac{|m|(m+k)}{|m|+|k|} \widehat{(\partial_1 h_0)}_{k-\ell} \widehat{h_0}_{\ell-m}(t) \widehat{\omega_0}_m e^{ikx_1} \\ &= \sum_{k,m\in\mathbb{Z}} i \operatorname{sgn}(k) \frac{|m|(m+k)(k-m)}{2(|m|+|k|)} \widehat{(h_0^2)}_{k-m}(t) \widehat{\omega_0}_m e^{ikx_1} \\ &= \frac{1}{2} \sum_{k,m\in\mathbb{Z}} i \operatorname{sgn}(k) |m|(|k|-|m|) \widehat{(h_0^2)}_{k-m}(t) \widehat{\omega_0}_m e^{ikx_1} = \frac{1}{2} \partial_1 (h_0^2 \Lambda \omega_0) + \frac{1}{2} H(h_0^2 \Lambda^2 \omega_0) \,. \end{split}$$

Therefore, we have that

$$\partial_{t}h_{2} - H\omega_{2} = \partial_{1}(\llbracket h_{1}, H \rrbracket H\omega_{0}) + \partial_{1}(\llbracket h_{0}, H \rrbracket H\omega_{1}) - \partial_{1}(\llbracket h_{0}, H \rrbracket \Lambda(h_{0}H\omega_{0}))$$

$$+ H[(\partial_{1}h_{0})\partial_{1}(h_{0}\omega_{0})] - H[(\partial_{1}h_{0})^{2}\omega_{0}] - \frac{1}{2}\partial_{1}(h_{0}^{2}\Lambda\omega_{0}) - \frac{1}{2}H(h_{0}^{2}\Lambda^{2}\omega_{0}), \quad (59a)$$

$$\partial_{t}\omega_{2} = -g\partial_{1}h_{2} + \partial_{1}[\partial_{t}h_{1}\partial_{t}h_{0} - \omega_{0}\omega_{1}] + \partial_{1}[\omega_{0}\partial_{t}h_{0}\partial_{1}h_{0}], \quad (59b)$$

We next time-differentiate (59a) and substitute (59b) to find that

$$\begin{split} \partial_t^2 h_2 + g \Lambda h_2 &= \partial_1 (\llbracket \partial_t h_1, H \rrbracket H \omega_0) + \partial_1 (\llbracket h_1, H \rrbracket H \partial_t \omega_0) + \partial_1 (\llbracket \partial_t h_0, H \rrbracket H \omega_1) \\ &+ \partial_1 (\llbracket h_0, H \rrbracket H \partial_t \omega_1) - \partial_1 (\llbracket \partial_t h_0, H \rrbracket \Lambda (h_0 H \omega_0)) \\ &- \partial_1 (\llbracket h_0, H \rrbracket \Lambda (\partial_t h_0 H \omega_0)) - \partial_1 (\llbracket h_0, H \rrbracket \Lambda (h_0 H \partial_t \omega_0)) \\ &+ H \big[(\partial_1 \partial_t h_0) \partial_1 (h_0 \omega_0) \big] + H \big[(\partial_1 h_0) \partial_1 (\partial_t h_0 \omega_0) \big] + H \big[(\partial_1 h_0) \partial_1 (h_0 \partial_t \omega_0) \big] \\ &- 2 H \big[(\partial_1 h_0) (\partial_1 \partial_t h_0) \omega_0 \big] - H \big[(\partial_1 h_0)^2 (\partial_t \omega_0) \big] - \partial_1 \big[h_0 (\partial_t h_0) (\Lambda \omega_0) \big] \\ &- \frac{1}{2} \partial_1 \big[h_0^2 (\Lambda \partial_t \omega_0) \big] - H \big[h_0 (\partial_t h_0) \Lambda^2 \omega_0 \big] - \frac{1}{2} H (h_0^2 \Lambda^2 \partial_t \omega_0) \\ &+ \Lambda \left[\partial_t h_1 \partial_t h_0 - \omega_0 \omega_1 \right] + \Lambda \left[\omega_0 \partial_t h_0 \partial_1 h_0 \right]. \end{split}$$

Thanks to the identities in (47), we conclude that

$$\omega_0 = -H\partial_t h_0$$
 and $\omega_1 = -H\partial_t h_1 + \Lambda(\llbracket h_0, H \rrbracket \partial_t h_0)$ on \mathbb{S}^1 .

Thus,

$$\begin{split} \partial_t^2 h_2 + g \Lambda h_2 &= \partial_1 \big([\![\partial_t h_1, H]\!] \partial_t h_0 \big) - g \partial_1 \big([\![h_1, H]\!] \Lambda h_0 \big) + \partial_1 \big([\![\partial_t h_0, H]\!] \big[\partial_t h_1 - \partial_1 \big([\![h_0, H]\!] \partial_t h_0 \big) \big] \big) \\ &+ \partial_1 \left([\![h_0, H]\!] \left[-g \Lambda h_1 + \frac{1}{2} \Lambda \big(|\partial_t h_0|^2 - |H \partial_t h_0|^2 \big) \right] \right) - \partial_1 \big([\![\partial_t h_0, H]\!] \Lambda \big(h_0 \partial_t h_0 \big) \big) \\ &- \partial_1 \big([\![h_0, H]\!] \Lambda \big((\partial_t h_0)^2 \big) \big) + g \partial_1 \big([\![h_0, H]\!] \Lambda \big(h_0 \Lambda h_0 \big) \big) \\ &- H \big[\big(\partial_1 \partial_t h_0 \big) \partial_1 \big(h_0 H \partial_t h_0 \big) \big] - H \big[\big(\partial_1 h_0 \big) \partial_1 \big(\partial_t h_0 H \partial_t h_0 \big) \big] - g H \big[\big(\partial_1 h_0 \big) \partial_1 \big(h_0 \partial_1 h_0 \big) \big] \\ &+ 2 H \big[\big(\partial_1 h_0 \big) \big(\partial_1 \partial_t h_0 \big) H \partial_t h_0 \big] + g H \big[\big(\partial_1 h_0 \big)^3 \big] - \partial_1 \big[h_0 \big(\partial_t h_0 \big) \big(\partial_1 \partial_t h_0 \big) \big] \\ &+ 2 H \big[h_0 \big(\Lambda \partial_1 h_0 \big) \big] - H \big[h_0 \big(\partial_t h_0 \big) \Lambda \partial_1 \partial_t h_0 \big] + \frac{g}{2} H \big(h_0^2 \Lambda^2 \partial_1 h_0 \big) \\ &+ \Lambda \big[\partial_t h_1 \partial_t h_0 + H \partial_t h_0 \big(-H \partial_t h_1 + \Lambda \big([\![h_0, H]\!] \partial_t h_0 \big) \big) \big] - \Lambda \big[H \partial_t h_0 \partial_t h_0 \partial_1 h_0 \big] \;. \end{split}$$

Using Tricomi's identity (49), we can reduce the previous expression to

$$\begin{split} \partial_t^2 h_2 + g \Lambda h_2 &= \partial_1 (\llbracket \partial_t h_1, H \rrbracket \partial_t h_0) - g \partial_1 (\llbracket h_1, H \rrbracket \Lambda h_0) + \partial_1 \big(\llbracket \partial_t h_0, H \rrbracket \big[\partial_t h_1 - \partial_1 \big(\llbracket h_0, H \rrbracket \partial_t h_0 \big) \big] \big) \\ &- \partial_1 \big(\llbracket h_0, H \rrbracket \big[g \Lambda h_1 - \partial_1 \big(\partial_t h_0 H \partial_t h_0 \big) \big] \big) - \partial_1 \big(\llbracket \partial_t h_0, H \rrbracket \Lambda \big(h_0 \partial_t h_0 \big) \big) \\ &- \partial_1 \big(\llbracket h_0, H \rrbracket \Lambda \big((\partial_t h_0)^2 \big) \big) + g \partial_1 \big(\llbracket h_0, H \rrbracket \Lambda \big(h_0 \Lambda h_0 \big) \big) \\ &- H \big[\big(\partial_1 \partial_t h_0 \big) \partial_1 \big(h_0 H \partial_t h_0 \big) \big] - H \big[\big(\partial_1 h_0 \big) \partial_1 \big(\partial_t h_0 H \partial_t h_0 \big) \big] - g H \big[\big(\partial_1 h_0 \big) \partial_1 \big(h_0 \partial_1 h_0 \big) \big] \\ &+ 2 H \big[\big(\partial_1 h_0 \big) \big(\partial_1 \partial_t h_0 \big) H \partial_t h_0 \big] + g H \big[\big(\partial_1 h_0 \big)^3 \big] - \partial_1 \big[h_0 \big(\partial_t h_0 \big) \big(\partial_1 \partial_t h_0 \big) \big] \\ &+ \frac{g}{2} \partial_1 \big[h_0^2 \big(\Lambda \partial_1 h_0 \big) \big] - H \big[h_0 \big(\partial_t h_0 \big) \Lambda \partial_1 \partial_t h_0 \big] + \frac{g}{2} H \big(h_0^2 \Lambda^2 \partial_1 h_0 \big) \\ &+ \Lambda \big[\partial_t h_1 \partial_t h_0 + H \partial_t h_0 \big(- H \partial_t h_1 + \Lambda \big(\llbracket h_0, H \rrbracket \partial_t h_0 \big) \big) \big] - \Lambda \big[H \partial_t h_0 \partial_t h_0 \partial_1 h_0 \big] \,. \end{split}$$

The cubic h-model follows from setting

$$h(x_1, t) = \epsilon h_0(x_1, t) + \epsilon^2 h_1(x_1, t) + \epsilon^3 h_2(x_1, t),$$

so that

$$\begin{split} \partial_t^2 h + g \Lambda h &= \epsilon^3 \bigg[\partial_1 \big(\llbracket \partial_t h_1, H \rrbracket \partial_t h_0 \big) - g \partial_1 \big(\llbracket h_1, H \rrbracket \Lambda h_0 \big) + \partial_1 \big(\llbracket \partial_t h_0, H \rrbracket \big[\partial_t h_1 - \partial_1 \big(\llbracket h_0, H \rrbracket \partial_t h_0 \big) \big] \big) \\ &- \partial_1 \big(\llbracket h_0, H \rrbracket \big[g \Lambda h_1 - \partial_1 \big(\partial_t h_0 H \partial_t h_0 \big) \big] \big) - \partial_1 \big(\llbracket \partial_t h_0, H \rrbracket \Lambda \big(h_0 \partial_t h_0 \big) \big) \\ &- \partial_1 \big(\llbracket h_0, H \rrbracket \Lambda \big((\partial_t h_0)^2 \big) \big) + g \partial_1 \big(\llbracket h_0, H \rrbracket \Lambda \big(h_0 \Lambda h_0 \big) \big) \\ &- H \big[\big(\partial_1 \partial_t h_0 \big) \partial_1 \big(h_0 H \partial_t h_0 \big) \big] - H \big[\big(\partial_1 h_0 \big) \partial_1 \big(\partial_t h_0 H \partial_t h_0 \big) \big] - g H \big[\big(\partial_1 h_0 \big) \partial_1 \big(h_0 \partial_1 h_0 \big) \big] \\ &+ 2 H \big[\big(\partial_1 h_0 \big) \big(\partial_1 \partial_t h_0 \big) H \partial_t h_0 \big] + g H \big[\big(\partial_1 h_0 \big)^3 \big] - \partial_1 \big[h_0 \big(\partial_t h_0 \big) \big(\partial_1 \partial_t h_0 \big) \big] \\ &+ \frac{g}{2} \partial_1 \big[h_0^2 \big(\Lambda \partial_1 h_0 \big) \big] - H \big[h_0 \big(\partial_t h_0 \big) \Lambda \partial_1 \partial_t h_0 \big] + \frac{g}{2} H \big(h_0^2 \Lambda^2 \partial_1 h_0 \big) \\ &+ \Lambda \left[\partial_t h_1 \partial_t h_0 + H \partial_t h_0 \left(- H \partial_t h_1 + \Lambda \big(\llbracket h_0, H \rrbracket \partial_t h_0 \big) \right) \right] - \Lambda \left[H \partial_t h_0 \partial_t h_0 \partial_1 h_0 \big] \bigg] \\ &+ \epsilon^2 \bigg[- \Lambda \big(|H \partial_t h_0|^2 \big) + g \Lambda \big(h_0 \Lambda h_0 \big) + g \partial_1 \big(h_0 \partial_1 h_0 \big) \bigg] \,. \end{split}$$

Then, we find that

$$\begin{split} \partial_t^2 h + g \Lambda h &= \partial_1 \big(\llbracket \epsilon^2 \partial_t h_1, H \rrbracket \epsilon \partial_t h_0 \big) - g \partial_1 \big(\llbracket h, H \rrbracket \epsilon \Lambda h_0 \big) + \partial_1 \big(\llbracket \epsilon \partial_t h_0, H \rrbracket \Big[\epsilon^2 \partial_t h_1 - \partial_1 \big(\llbracket h, H \rrbracket \partial_t h \big) \Big] \big) \\ &- \partial_1 \big(\llbracket \epsilon h_0, H \rrbracket \Big[g \Lambda \epsilon^2 h_1 - \partial_1 \big(\partial_t h H \partial_t h \big) \Big] \big) - \partial_1 \big(\llbracket \partial_t h, H \rrbracket \Lambda (h \partial_t h) \big) \\ &- \partial_1 \big(\llbracket h, H \rrbracket \Lambda ((\partial_t h)^2) \big) + g \partial_1 \big(\llbracket h, H \rrbracket \Lambda (h \Lambda h) \big) \\ &- H \Big[(\partial_1 \partial_t h) \partial_1 (h H \partial_t h) \Big] - H \Big[(\partial_1 h) \partial_1 (\partial_t h H \partial_t h) \Big] - g H \Big[(\partial_1 h) \partial_1 (h \partial_1 h) \Big] \\ &+ 2 H \Big[(\partial_1 h) (\partial_1 \partial_t h) H \partial_t h \Big] + g H \Big[(\partial_1 h)^3 \Big] - \partial_1 \Big[h (\partial_t h) (\partial_1 \partial_t h) \Big] \\ &+ \frac{g}{2} \partial_1 \Big[h^2 (\Lambda \partial_1 h) \Big] - H \Big[h (\partial_t h) \Lambda \partial_1 \partial_t h \Big] - \frac{g}{2} H (h^2 \partial_1^3 h) \\ &+ \Lambda \left[\epsilon^2 \partial_t h_1 \epsilon \partial_t h_0 + H \epsilon \partial_t h_0 \left(-H \partial_t h + \Lambda \left(\llbracket h, H \rrbracket \partial_t h \right) \right) \right] - \Lambda \left[H \partial_t h \partial_t h \partial_1 h \right] + O(\epsilon^4) \,. \end{split}$$

We observe that

$$-g\partial_1(\llbracket h, H \rrbracket \epsilon \Lambda h_0) - g\partial_1\left(\llbracket \epsilon h_0, H \rrbracket \Lambda \epsilon^2 h_1\right) = -g\partial_1\left(\llbracket h, H \rrbracket \Lambda h\right) + O(\epsilon^4);$$

thus, we can simplify the equation as follows:

$$\begin{split} \partial_t^2 h + g \Lambda h &= \partial_1 \big(\llbracket \epsilon^2 \partial_t h_1, H \rrbracket \epsilon \partial_t h_0 \big) - g \partial_1 \left(\llbracket h, H \rrbracket \Lambda h \big) + \partial_1 \big(\llbracket \epsilon \partial_t h_0, H \rrbracket \Big[\epsilon^2 \partial_t h_1 - \partial_1 \big(\llbracket h, H \rrbracket \partial_t h \big) \Big] \big) \\ &+ \partial_1 \left(\llbracket h, H \rrbracket \left[\partial_1 \big(\partial_t h H \partial_t h \big) \right] \right) - \partial_1 \big(\llbracket \partial_t h, H \rrbracket \Lambda (h \partial_t h) \big) \\ &- \partial_1 \big(\llbracket h, H \rrbracket \Lambda ((\partial_t h)^2) \big) + g \partial_1 \big(\llbracket h, H \rrbracket \Lambda (h \Lambda h) \big) \\ &- H \Big[(\partial_1 \partial_t h) \partial_1 (h H \partial_t h) \Big] - H \Big[(\partial_1 h) \partial_1 (\partial_t h H \partial_t h) \Big] - g H \Big[(\partial_1 h) \partial_1 (h \partial_1 h) \Big] \\ &+ 2 H \Big[(\partial_1 h) (\partial_1 \partial_t h) H \partial_t h \Big] + g H \Big[(\partial_1 h)^3 \Big] - \partial_1 \Big[h (\partial_t h) (\partial_1 \partial_t h) \Big] \\ &+ \frac{g}{2} \partial_1 \Big[h^2 (\Lambda \partial_1 h) \Big] - H \Big[h (\partial_t h) \Lambda \partial_1 \partial_t h \Big] - \frac{g}{2} H (h^2 \partial_1^3 h) \\ &+ \Lambda \left[\epsilon^2 \partial_t h_1 \epsilon \partial_t h_0 + H \epsilon \partial_t h_0 \left(-H \partial_t h + \Lambda \left(\llbracket h, H \rrbracket \partial_t h \right) \right) \right] - \Lambda \left[H \partial_t h \partial_t h \partial_1 h \right] + O(\epsilon^4) \,. \end{split}$$

We also compute that

$$\partial_1(\llbracket \epsilon^2 \partial_t h_1, H \rrbracket \epsilon \partial_t h_0) = \partial_1(\llbracket \epsilon^2 \partial_t h_1, H \rrbracket \partial_t h) + O(\epsilon^4),$$

$$\Lambda \left[\epsilon^2 \partial_t h_1 \epsilon \partial_t h_0 \right] = \Lambda \left[\epsilon^2 \partial_t h_1 \partial_t h \right] + O(\epsilon^4) ,
\partial_1 \left(\left[\epsilon \partial_t h_0, H \right] \epsilon^2 \partial_t h_1 \right) = \partial_1 \left(\left[\partial_t h, H \right] \epsilon^2 \partial_t h_1 \right) + O(\epsilon^4) ,$$

so that

$$\partial_{1}(\llbracket \epsilon^{2}\partial_{t}h_{1}, H \rrbracket \epsilon \partial_{t}h_{0}) + \Lambda \left[\epsilon^{2}\partial_{t}h_{1}\epsilon \partial_{t}h_{0} \right] + \partial_{1}(\llbracket \epsilon \partial_{t}h_{0}, H \rrbracket \epsilon^{2}\partial_{t}h_{1})
= \partial_{1}(\llbracket \epsilon^{2}\partial_{t}h_{1}, H \rrbracket \partial_{t}h) + \Lambda \left[\epsilon^{2}\partial_{t}h_{1}\partial_{t}h \right] + \partial_{1}(\llbracket \partial_{t}h, H \rrbracket \epsilon^{2}\partial_{t}h_{1}) + O(\epsilon^{4})
= \partial_{1}(\epsilon^{2}\partial_{t}h_{1}H\partial_{t}h) + \partial_{1}(\llbracket \partial_{t}h, H \rrbracket \epsilon^{2}\partial_{t}h_{1}) + O(\epsilon^{4})
= \partial_{1}(\epsilon^{2}\partial_{t}h_{1}H\partial_{t}h) + \partial_{1}(\partial_{t}hH\epsilon^{2}\partial_{t}h_{1}) - \Lambda \left[\epsilon^{2}\partial_{t}h_{1}\partial_{t}h \right] + O(\epsilon^{4}). (60)$$

Using Tricomi's identity for two functions, we find that

$$\partial_1(\epsilon^2 \partial_t h_1 H \partial_t h) + \partial_1(\partial_t h H \epsilon^2 \partial_t h_1) = -\Lambda \left[H \partial_t h \epsilon^2 H \partial_t h_1 - \partial_t h \epsilon^2 \partial_t h_1 \right]. \tag{61}$$

Grouping terms further using (60) and (61), together with

$$-\Lambda \left[H\epsilon \partial_t h_0 H \partial_t h \right] = -\Lambda \left[(H\partial_t h)^2 \right] + \Lambda \left[H\epsilon^2 \partial_t h_1 H \partial_t h \right] + O(\epsilon^4)$$

we obtain that

$$\begin{split} \partial_{1}(\epsilon^{2}\partial_{t}h_{1}H\partial_{t}h) + \partial_{1}\left(\partial_{t}hH\epsilon^{2}\partial_{t}h_{1}\right) - \Lambda\left[\epsilon^{2}\partial_{t}h_{1}\partial_{t}h\right] - \Lambda\left[H\epsilon\partial_{t}h_{0}H\partial_{t}h\right] \\ &= -\Lambda\left[H\partial_{t}h\epsilon^{2}H\partial_{t}h_{1} - \partial_{t}h\epsilon^{2}\partial_{t}h_{1}\right] - \Lambda\left[\epsilon^{2}\partial_{t}h_{1}\partial_{t}h\right] \\ &- \Lambda\left[\left(H\partial_{t}h\right)^{2}\right] + \Lambda\left[H\epsilon^{2}\partial_{t}h_{1}H\partial_{t}h\right] + O(\epsilon^{4}) \,. \end{split}$$

The cubic h-model is then given by

$$\begin{split} \partial_t^2 h + g \Lambda h &= -\Lambda \big[\left(H \partial_t h \right)^2 \big] - g \partial_1 \left(\llbracket h, H \rrbracket \Lambda h \right) - \partial_1 \left(\llbracket \partial_t h, H \rrbracket \left[\partial_1 \left(\llbracket h, H \rrbracket \partial_t h \right) \right] \right) \\ &+ \partial_1 \left(\llbracket h, H \rrbracket \left[\partial_1 \left(\partial_t h H \partial_t h \right) \right] \right) - \partial_1 \left(\llbracket \partial_t h, H \rrbracket \Lambda \left(h \partial_t h \right) \right) \\ &- \partial_1 \left(\llbracket h, H \rrbracket \Lambda \left(\left(\partial_t h \right)^2 \right) \right) + g \partial_1 \left(\llbracket h, H \rrbracket \Lambda \left(h \Lambda h \right) \right) \\ &- H \big[\left(\partial_1 \partial_t h \right) \partial_1 \left(h H \partial_t h \right) \right] - H \big[\left(\partial_1 h \right) \partial_1 \left(\partial_t h H \partial_t h \right) \right] - g H \big[\left(\partial_1 h \right) \partial_1 \left(h \partial_1 h \right) \right] \\ &+ 2 H \big[\left(\partial_1 h \right) \left(\partial_1 \partial_t h \right) H \partial_t h \right] + g H \big[\left(\partial_1 h \right)^3 \big] - \partial_1 \big[h \left(\partial_t h \right) \left(\partial_1 \partial_t h \right) \big] \\ &+ \frac{g}{2} \partial_1 \big[h^2 \left(\Lambda \partial_1 h \right) \big] - H \big[h \left(\partial_t h \right) \Lambda \partial_1 \partial_t h \right] - \frac{g}{2} H \left(h^2 \partial_1^3 h \right) \\ &+ \Lambda \left[H \partial_t h \Lambda \left(\llbracket h, H \rrbracket \partial_t h \right) \right] - \Lambda \left[H \partial_t h \partial_t h \partial_1 h \right] \right] \,. \end{split}$$

Therefore,

$$\partial_t^2 h + g\Lambda h = -\Lambda [(H\partial_t h)^2] + g\partial_1 (h\partial_1 h) + g\Lambda (h\Lambda h) + Q(h).$$
 (62)

Making use of the commutator identities in Appendix A, the cubic nonlinearity Q(h) can be written as

$$Q(h) = -\partial_{1} \left[[\partial_{t}h, H] \partial_{1} (hH\partial_{t}h) - [h, H] \partial_{1} ([\partial_{t}h, H] \partial_{t}h) - g[h, H] \Lambda (h\Lambda h) \right]$$

$$+ H \left[(h\partial_{t}h)(\Lambda\partial_{t}h) - \frac{g}{2} [h^{2}, H] \partial_{1}^{2}h + h\partial_{t}h\partial_{1}\partial_{t}h \right]$$

$$- H \left[(H\partial_{t}h)\Lambda (hH\partial_{t}h) - H \left[(H\partial_{t}h)h(\partial_{1}\partial_{t}h) \right] \right].$$

$$(63)$$

6 Well-posedness of the h-models

We study local well-posedness in Wiener spaces (10) for the quadratic h-model (51) and the cubic h-model (62).

In the case of the quadratic h-model (51), local well-posedness for analytic data can be established using the Cauchy-Kowalewski theorem of Schneider & Wayne [71] (see also [63, 64, 67]). However, the nonlinearity of the cubic h-model (62) is not directly suitable for such an approach, due to terms containing three derivatives. While it may be possible that the Cauchy-Kowalewski theorem can again be applied to the cubic h-model, either by some further simplification of the cubic nonlinearity or by a modification of the proof of the Cauchy-Kowalewski theorem, we have provided a different proof of well-posedness that also works for nonlinearities with higher-order derivatives, and hence could be used for even higher-order truncations of the Stokes expansion. Moreover, our method of proof also provides the convergence of the Stokes expansion (25)–(26), which is of fundamental importance to consequent error analysis. Such convergence does not directly follow from the application of the Cauchy-Kowalewski theorem, but rather from a succession of inequalities leading to a uniform radius of convergence for the power series.

Specifically, our method of proof relies upon the linear recursion derived in Equations (111) and (112) in Appendix B. For the Navier-Stokes equations, the idea of using the summability of an asymptotic expansion to prove well-posedness goes back to Oseen [65] and Knightly [49]; however, for parabolic-type problems, the summability follows from the diffusive properties of the Stokes semigroup. For hyperbolic wave equations with no diffusion set on a spatially periodic domain (and hence without dispersive decay), a different approach to summability must be established. For the h-models, summability of the Stokes expansion follows from bounds of the nonlinearity at each step of the recursion relation. We show that the X_{τ} -norms (10) have bounds that grow like the Catalan numbers $\{C_k\}_{k=0}^{\infty}$, which can be defined recursively as

$$C_k = \sum_{j=0}^{k-1} C_j C_{k-1-j}, \qquad C_0 = 1.$$
 (64)

This idea of using the structure of the nonlinearity and the Catalan numbers is, to the best of our knowledge, new to the analysis of water waves models.

We remark that a closely related two-fluid asymptotic model derived in [38] has been shown to be well-posed in Sobolev spaces when the initial data satisfies a certain sign condition. In particular, in the case that $\partial_t h|_{t=0} < 0$ for each point on the free-surface, that model is locally well-posed for arbitrary data and globally well-posed under certain size restrictions (see Theorems 7.1 and 7.6 in [38]).² It is possible that the quadratic h-model is also well-posed in Sobolev spaces when this sign condition holds for the initial data, and we plan to investigate this in future work.

²The condition $\partial_t h < 0|_{t=0}$ can occur globally with certain in-flow boundary conditions.

6.1 Well-posedness theory for the quadratic h-model

Well-posedness of the quadratic h-model can be established using the Cauchy-Kowalewski theorem in [71]. We state this result as follows:

Theorem 3. Let $\epsilon > 0$, g > 0 and the initial data in (27) $(h_{\text{init}}, \dot{h}_{\text{init}}) \in X_1 \times X_1$ be given. Then there exists a unique analytic solution $h(x_1, t) \in C([0, T]; X_{0.5})$ to (51) for t in the time interval [0, T] with

$$T = \frac{1}{4\epsilon}$$
.

Equivalently, the Stokes expansion for the quadratic h-model (51) converges for arbitrary $\epsilon > 0$ and T > 0 taken sufficiently small.

We provide a proof in Appendix B using the summability of the recursion relation. Note that we simultaneously prove that the Stokes expansion converges.

6.2 Well-posedness theory for the cubic h-model

As we have seen, the cubic h-model can be written as the following nonlinear wave equation (62) where Q(h) is defined in (63). Using the ansatz (25), the cubic h-model (62) can be written as

$$\partial_t^2 \widetilde{h} = -g\Lambda \widetilde{h} - \epsilon \Lambda (H\partial_t \widetilde{h})^2 + g\epsilon \left(\partial_1 (\widetilde{h}\partial_1 \widetilde{h}) + \Lambda (\widetilde{h}\Lambda \widetilde{h}) \right) + \epsilon^2 \mathcal{Q}(\widetilde{h}), \tag{65}$$

with initial conditions (28). We again consider the expansion $\tilde{h}(x_1,t) = h_0(x_1,t) + \epsilon h_1(x_1,t) + \epsilon^2 h_2(x_1,t) + \cdots$. The quadratic nonlinearity follows as in (109). It thus suffices to expand the cubic nonlinearity. We define

$$Q(h_{r}, h_{j-r}, h_{k-2-j}) = -\partial_{1} \left[[\![\partial_{t}h_{r}, H]\!] \partial_{1} (h_{j-r}H\partial_{t}h_{k-2-j}) - [\![h_{r}, H]\!] \partial_{1} ([\![\partial_{t}h_{j-r}, H]\!] \partial_{t}h_{k-2-j}) \right]$$

$$- g[\![h_{r}, H]\!] \Lambda(h_{j-r}\Lambda h_{k-2-j}) + H[(h_{r}\partial_{t}h_{j-r})(\Lambda\partial_{t}h_{k-2-j})]$$

$$- \frac{g}{2} [\![h_{r}h_{j-r}, H]\!] \partial_{1}^{2}h_{k-2-j} + h_{r}\partial_{t}h_{j-r}\partial_{1}\partial_{t}h_{k-2-j}$$

$$- H[(H\partial_{t}h_{r})\Lambda(h_{j-r}H\partial_{t}h_{k-2-j})]$$

$$- H[(H\partial_{t}h_{r})h_{j-r}(\partial_{1}\partial_{t}h_{k-2-j})]$$

$$(66)$$

Comparing powers of ϵ , we find that

$$\partial_{t}^{2}h_{k} = -g\Lambda h_{k} + \sum_{j=0}^{k-1} \left(\Lambda \left[gh_{j}\Lambda h_{k-1-j} - H\partial_{t}h_{j}H\partial_{t}h_{k-1-j} \right] + g\partial_{1} \left[h_{j}\partial_{1}h_{k-1-j} \right] \right) + \sum_{j=0}^{k-2} \sum_{r=0}^{j} \mathcal{Q}(h_{r}, h_{j-r}, h_{k-2-j}),$$

$$(67)$$

with initial conditions (110)

Our starting point is the linear recursion (67) and (66). Similarly, the solution to (67) for k > 0 verifies

$$\hat{h}_k(\ell, t) = \frac{1}{\sqrt{g|\ell|}} \int_0^t f(\ell, s) \sin\left(\sqrt{g|\ell|}(t - s)\right) ds, \qquad (68)$$

and

$$\partial_t \hat{h}_k(\ell, t) = \int_0^t f(\ell, s) \cos\left(\sqrt{g|\ell|}(t - s)\right) ds, \qquad (69)$$

where f is the Fourier transform of the (linear) forcing

$$\check{f} = \sum_{j=0}^{k-1} \left(\Lambda \left[h_j \Lambda h_{k-1-j} - H \partial_t h_j H \partial_t h_{k-1-j} \right] + g \partial_1 \left[h_j \partial_1 h_{k-1-j} \right] \right)
+ \sum_{j=0}^{k-2} \sum_{r=0}^{j} \mathcal{Q}(h_r, h_{j-r}, h_{k-2-j}),$$
(70)

where Q is given by (66).

Theorem 4. Let $\epsilon > 0$, g > 0 and the initial data in (27) $(h_{\text{init}}, \dot{h}_{\text{init}}) \in X_1 \times X_1$ be given. Then there exists a unique analytic solution

$$h(x_1, t) \in C([0, T]; X_{0.5})$$

to (62) for t in the time interval [0,T] with

$$T < \min\left\{\frac{1}{8\epsilon}, 1\right\}$$
.

Equivalently, the Stokes expansion for the cubic h-model (62) converges for arbitrary $\epsilon > 0$ and T > 0 taken sufficiently small.

Proof. The proof of this Theorem is similar to the proof of Theorem 3 in Appendix B. As before, we fix $1 < R \in \mathbb{Z}^+$ and consider $0 < k \leqslant R$. We need to estimate $\|\mathcal{Q}(h_r, h_{j-r}, h_{k-2-j})\|_{X_{R+1-k}}$. Following Theorem 3 in Appendix B together with (119) and the trivial identity

$$|\ell| \le |\ell - m| + |m| \le |\ell - m| + |m - n| + |n|,$$

we have that

$$\begin{split} \|\mathcal{Q}(h_r,h_{j-r},h_{k-2-j})\|_{X_{R+1-k}} &\leqslant c_1(g) \bigg[\|\partial_t h_r\|_{X_{R+2-k}} \|h_{j-r}\|_{X_{R+2-k}} \|\partial_t h_{k-2-j}\|_{X_{R+2-k}} \\ &+ \|h_r\|_{X_{R+2-k}} \|h_{j-r}\|_{X_{R+2-k}} \|h_{k-2-j}\|_{X_{R+2-k}} \\ &+ \|h_r\|_{X_{R+2-k}} \|\partial_t h_{j-r}\|_{X_{R+2-k}} \|\partial_t h_{k-2-j}\|_{X_{R+2-k}} \bigg] \,. \end{split}$$

As before, we have that, for $r \leq j \leq k-2$

$$R + 2 - k = R - (k - 2) \le R + 1 - r,$$

$$R + 2 - k \le R + 1 - j + r = R + 1 - (j - r),$$

$$R + 2 - k \le R + 1 - (k - 2 - j).$$

Thus, we can estimate

$$\begin{split} \|\mathcal{Q}(h_r,h_{j-r},h_{k-2-j})\|_{X_{R+1-k}} &\leqslant c_1(g) \bigg[\|\partial_t h_r\|_{X_{R+1-r}} \|h_{j-r}\|_{X_{R+1-(j-r)}} \|\partial_t h_{k-2-j}\|_{X_{R+1-(k-2-j)}} \\ &+ \|h_r\|_{X_{R+1-r}} \|h_{j-r}\|_{X_{R+1-(j-r)}} \|h_{k-2-j}\|_{X_{R+1-(k-2-j)}} \\ &+ \|h_r\|_{X_{R+1-r}} \|\partial_t h_{j-r}\|_{X_{R+1-(j-r)}} \|\partial_t h_{k-2-j}\|_{X_{R+1-(k-2-j)}} \bigg] \,. \end{split}$$

Recalling (120), we find that

$$\begin{split} \|h_k(t)\|_{X_{R+1-k}} + \|\partial_t h_k(t)\|_{X_{R+1-k}} \\ &\leqslant c_2(g) \int_0^t \bigg[\sum_{j=0}^{k-1} \bigg[\|\partial_t h_j(s)\|_{X_{R+1-j}} \|\partial_t h_{k-1-j}(s)\|_{X_{R+1-(k-1-j)}} \\ &+ \|h_j(s)\|_{X_{R+1-j}} \|h_{k-1-j}(s)\|_{X_{R+1-(k-1-j)}} \bigg] \\ &+ \sum_{j=0}^{k-2} \sum_{r=0}^{j} \bigg[\|\partial_t h_r\|_{X_{R+1-r}} \|h_{j-r}\|_{X_{R+1-(j-r)}} \|\partial_t h_{k-2-j}\|_{X_{R+1-(k-2-j)}} \\ &+ \|h_r\|_{X_{R+1-r}} \|h_{j-r}\|_{X_{R+1-(j-r)}} \|h_{k-2-j}\|_{X_{R+1-(k-2-j)}} \\ &+ \|h_r\|_{X_{R+1-r}} \|\partial_t h_{j-r}\|_{X_{R+1-(j-r)}} \|\partial_t h_{k-2-j}\|_{X_{R+1-(k-2-j)}} \bigg] \bigg] \, ds \, . \end{split}$$

We define

$$\mathscr{A}_k(t) = \max \left\{ c_2(g), 1 \right\} \left[\|h_k(t)\|_{X_{R+1-k}} + \|\partial_t h_k(t)\|_{X_{R+1-k}} \right].$$

Then, we can conclude that

$$\mathscr{A}_{k}(t) \leqslant \int_{0}^{t} \sum_{j=0}^{k-1} \mathscr{A}_{k-1-j}(s) \mathscr{A}_{j}(s) + \sum_{j=0}^{k-2} \sum_{r=0}^{j} \mathscr{A}_{k-2-j}(s) \mathscr{A}_{j-r}(s) \mathscr{A}_{r}(s) ds, \ \mathscr{A}_{0} = 1.$$

We assume that t < 1. Recalling that for the Catalan numbers (64) we have that

$$\sum_{j=0}^{k-2} \sum_{r=0}^{j} C_r C_{j-r} C_{k-2-j} = \sum_{j=0}^{k-2} C_{j+1} C_{k-1-(j+1)}$$

$$= \sum_{n=1}^{k-1} C_n C_{k-1-n}$$

$$\leq \sum_{n=1}^{k-1} C_n C_{k-1-n} + C_0 C_{k-1}$$

$$\leq C_k,$$

we can prove by induction that

$$\mathscr{A}_k \leqslant 2^k \mathcal{C}_k t^{k+1}$$
.

Using this bound, we can conclude the existence and uniqueness as in Theorem 3 in Appendix B. $\ \Box$

7 The Craig-Sulem WW2 model

Zakharov [84] formulated the water waves problem as the following system of one-dimensional nonlinear and nonlocal equations:

$$\partial_t h = G(h)\Psi \tag{71a}$$

$$\partial_t \Psi = -gh - \frac{1}{2} |\partial_1 \Psi|^2 + \frac{1}{2} \frac{(\partial_1 h \partial_1 \Psi + G(h) \Psi)^2}{1 + |\partial_1 h|^2}, \tag{71b}$$

where $h(x_1, t)$ is the free surface, $\Psi(x_1, t)$ is the trace of the velocity potential $\mathbf{u} = \nabla \phi$ on the free surface

$$\Psi(x_1, t) = \phi(x_1, h(x_1, t), t),$$

and G(h) is the Dirichlet-Neumann operator

$$G(h)\Psi(x_1,t) = \frac{\partial \phi}{\partial x_2}\Big|_{(x_1,h(x_1,t),t)} - \partial_1 h(x_1,t) \frac{\partial \phi}{\partial x_1}\Big|_{(x_1,h(x_1,t),t)}.$$
 (72)

As a way to numerically simulate the evolution of water waves when surface tension is neglected, Craig and Sulem [31] gave a power series expansion for the Dirichlet-to-Neumann operator (72) as³

$$G(h) = \sum_{j=0}^{\infty} G_j(h), \tag{73}$$

with

$$G_0 = \Lambda,$$

$$G_j(h) = -\Lambda^{j-1} \partial_1 \frac{h^j}{j!} \partial_1 - \sum_{i=0}^{j-1} \Lambda^{j-i} \frac{h^{j-i}}{(j-i)!} G_i(h).$$

By keeping terms up to certain order in the previous expansion (73) and starting from the Zakharov formulation (71), Craig and Sulem obtained a hierarchy of new truncated series models of the water waves problem. For instance, when we keep the terms up to second order, G_0 and G_1 , we obtain the WW2 (water waves 2) system

$$\partial_t h = \Lambda \Psi - \partial_1 (\llbracket H, h \rrbracket \Lambda \Psi) \tag{74a}$$

$$\partial_t \Psi = -gh + \frac{1}{2} \left((\Lambda \Psi)^2 - (\partial_1 \Psi)^2 \right). \tag{74b}$$

³This type of expansion for the Dirichlet-to-Neumann operator was first used in electromagnetism by Milder [56] and Milder & Sharp [57].

We define

$$\omega(x_1, t) = \epsilon \omega_0(x_1, t) + \epsilon^2 \omega_1(x_1, t). \tag{75}$$

Similarly, defining h, ω as in (50) and (75), respectively, and using (47) we have that

$$\frac{1}{2}\partial_1(|\partial_t h_0|^2 - |\omega_0|^2) = \frac{1}{2}\partial_1(|H\omega_0|^2 - |\omega_0|^2).$$

Then, neglecting terms of order $O(\epsilon^3)$, from (47) we obtain the following coupled transport equations

$$\partial_t h = H\omega + \partial_1 \left(\llbracket h, H \rrbracket H\omega \right) , \tag{76a}$$

$$\partial_t \omega = -g \partial_1 h + \Lambda(\omega H \omega). \tag{76b}$$

These equations are the WW2 system obtained by Craig & Sulem writen in the variable $\omega = \partial_1 \Psi$. Thus, our method is also able to recover the WW2 system. Following the proof of Theorem 4, we can establish the following result for the WW2 Craig-Sulem system:

Theorem 5. Let g > 0 and the initial data $(h_{\text{init}}, \omega_{\text{init}}) \in X_1 \times X_1$ be given. Then there exists a unique analytic solution $(h(x_1, t), \omega(x_1, t))$ to (76) for t in the time interval [0, T] with 0 < T small enough.

In the following we are going to write the WW2 Craig-Sulem model as a wave equation. For an arbitrary function f, we define the operator

$$\mathscr{T}f = \partial_1 \llbracket H, h \rrbracket f.$$

The following inequalities hold

$$\begin{split} &\|\mathcal{T}f\|_{L^{2}}\leqslant C\|\partial_{1}h\|_{\dot{H}^{1}}\|f\|_{L^{2}},\\ &\|\mathcal{T}^{2}f\|_{L^{2}}\leqslant C\|\partial_{1}h\|_{\dot{H}^{1}}\|\mathcal{T}f\|_{L^{2}}\leqslant (C\|\partial_{1}h\|_{\dot{H}^{1}})^{2}\|f\|_{L^{2}},\\ &\|\mathcal{T}^{k}f\|_{L^{2}}\leqslant C\|\partial_{1}h\|_{\dot{H}^{1}}\|\mathcal{T}^{k-1}f\|_{L^{2}}\leqslant \ldots\leqslant (C\|\partial_{1}h\|_{\dot{H}^{1}})^{k}\|f\|_{L^{2}}. \end{split}$$

We define the following Neumann series

$$\mathscr{N} = \sum_{k=0}^{\infty} \mathscr{T}^k.$$

Then, if $\|\partial_1 h\|_{\dot{H}^1}C < 1$ we have that

$$\|\mathscr{N}f\|_{L^2} \le \|f\|_{L^2} \sum_{k=0}^{\infty} (C\|\partial_1 h\|_{L^2})^k \le \widetilde{C}(\|\partial_1 h\|_{L^2})\|f\|_{L^2},$$

so, denoting by where I the identity operator, we have that $I-\mathscr{T}$ is invertible and

$$(I - \mathcal{T})^{-1} = \mathcal{N}.$$

We observe that (76a) is equivalent to

$$(I - \mathcal{T})^{-1} \partial_t h = H\omega$$

Using the previous operators, we find the following equivalent formulation of the Craig-Sulem WW2 model as a nonlinear wave equation:

$$\partial_t^2 h = -g\Lambda h + \partial_1(\partial_t h H \partial_t h) - \partial_1 \llbracket H, \partial_t h \rrbracket \partial_t h + g\partial_1 \llbracket H, h \rrbracket \Lambda h + \mathcal{P}$$
(77)

where the cubic and higher nonlinearities are contained in

$$\mathcal{P} = \partial_1 \left(H \partial_t h \mathcal{M} \partial_t h \right) + \partial_1 \left(H \mathcal{M} \partial_t h \left(\partial_t h + \mathcal{M} \partial_t h \right) \right) - \partial_1 \left(\llbracket H, \partial_t h \rrbracket \left(\mathcal{M} h_t \right) \right) + \partial_1 \left(\llbracket H, h \rrbracket \left(\partial_1 \left(\left(-H \partial_t h - H \mathcal{M} \partial_t h \right) \left(\partial_t h + \mathcal{M} \partial_t h \right) \right) \right) , \tag{78}$$

and the operator \mathcal{M} is defined as

$$\mathscr{M} = \sum_{k=1}^{\infty} \partial_1 \llbracket H, h \rrbracket^k.$$

In particular, we observe that, when the cubic and higher nonlinearities in \mathcal{P} are neglected, the Craig-Sulem WW2 model reduces to the quadratic h-model (51) (or the, so-called, "Model" by Akers and Milewski [2]). Note that in [9], the authors suggest that the Craig-Sulem models may be unreliable for numerical simulation.

8 Estimating the difference between the h-models and the solution of the full water waves problem

In this section we estimate the error of solutions of the h-models to solutions of the full water waves system.

Let $(h_{\text{init}}, \dot{h}_{\text{init}})$ be a $\mathcal{O}(\epsilon)$ initial data and consider its corresponding local solution to the full water waves problem (h^{ww}, ω^{ww}) in $C([0,T]; X_1)$. As we described in the introduction, the well-posedness of the water waves problem is well-known (see the works by Ovsjannikov [66] and Shinbrot [74] for the case with analytic initial data), and that solutions exists for a lifespan $T = \mathcal{O}(\epsilon^{-1})$. We have the following

Theorem 6. Let $\epsilon > 0$, g > 0 and the initial data $(h_{\text{init}}, \dot{h}_{\text{init}}) \in X_1 \times X_1$ be given. Denote by (h^{ww}, ω^{ww}) the local solution in $C([0, T(\epsilon)]; X_1)$ of the full water waves problem starting from the initial data $(h_{\text{init}}, \dot{h}_{\text{init}})$ and let h^{qm} denote the solution to the quadratic h-model (51). Then, as long as both solutions exist,

$$||h^{ww} - h^{qm}||_{C([0,T]:X_{0.5})} \le \mathcal{O}(\epsilon^3).$$

Proof. From [66] and [74], there exists analytic solutions to the full water waves problem; hence, we write the solution h^{ww} as an asymptotic series We have that

$$h^{ww}(x_1, t) = \epsilon \sum_{j=0}^{\infty} \epsilon^j h_j^{ww}(x_1, t).$$

$$(79)$$

It follows that each term h_j evolves according to (31), (32) and (34). We have also shown that

$$h^{qm}(x_1,t) = \epsilon \sum_{j=0}^{\infty} \epsilon^j h_j^{qm}(x_1,t), \tag{80}$$

with h_i^{qm} evolving according to (109).

It follows from (79) that

$$\sup_{0 \leqslant t \leqslant T} \|h^{ww} - \epsilon \sum_{j=0}^{1} \epsilon^{j} h_{j}^{ww}\|_{X_{0.5}} \leqslant \mathcal{O}(\epsilon^{3}),$$

and from (80),

$$\sup_{0 \leqslant t \leqslant T} \|h^{qm} - \epsilon \sum_{j=0}^{1} \epsilon^{j} h_{j}^{qm}\|_{X_{0.5}} \leqslant \mathcal{O}(\epsilon^{3}).$$

We have to estimate

$$\| \sum_{j=0}^{1} \epsilon^{j} h_{j}^{ww} - \sum_{j=0}^{1} \epsilon^{j} h_{j}^{qm} \|_{X_{0.5}}.$$

From (109) and (47), we have that

Analogously, we have that

$$h_0^{ww} - h_0^{qm} = 0 \,,$$

and from (48b) and (109), we also have that

$$h_1^{ww} - h_1^{qm} = 0.$$

Thus, the terms in each series only begin to deviate at $O(\epsilon^3)$, which establishes the result. \Box

Theorem 7. Let $\epsilon > 0$, g > 0 and the initial data $(h_{\text{init}}, \dot{h}_{\text{init}}) \in X_1 \times X_1$ be given. Denote by (h^{ww}, ω^{ww}) the local solution in $C([0, T(\epsilon)]; X_1)$ of the full water waves problem starting from the initial data $(h_{\text{init}}, \dot{h}_{\text{init}})$ and let h^{cm} denote the solution to the cubic h-model (62). Then, as long as both solutions exist,

$$||h^{ww} - h^{cm}||_{C([0,T],X_{0.5})} \le \mathcal{O}(\epsilon^4).$$

Proof. The proof follows as in Theorem 6 by noting that for the cubic h-model

$$h_2^{ww} - h_2^{cm} = 0 \,,$$

and hence the deviation in the series representations of the two solutions occurs at $O(\epsilon^4)$. \Box

9 Numerical comparison of water waves and the h-model

In this section we compute solutions of the quadratic and cubic h-models and compare them to numerical solutions of the Euler equations. We find that the linear, quadratic and cubic h-models converge at the expected rates as $\epsilon \to 0$, and show regimes where the quadratic model captures the essential features of the wave beyond the linear regime, and where the cubic model captures features beyond the quadratic regime. We also observe that the quadratic model can form corner singularities in finite time, while the cubic model can evolve to an unstable state where high-frequency Fourier modes of the solution start growing rapidly. This only causes problems for large-amplitude waves on excessively fine grids.

9.1 Solving the Euler equations

To evolve the full water wave equations, we use the spectrally accurate boundary integral method developed by Wilkening [78] and Wilkening and Yu [79] for computing standing water waves. While a conformal mapping approach [33, 34, 58] is usually easier to implement, the result would have to be re-parametrized to be equally-spaced in x in order to compare with the h-model. This is not particularly difficult, but the boundary integral method is more natural in this setting. We write the Euler equations in the form

$$h_t = \phi_y - h_x \phi_x,$$

$$\varphi_t = P \left[\phi_y h_t - \frac{1}{2} \phi_x^2 - \frac{1}{2} \phi_y^2 - gh + \frac{\lambda}{\rho} \partial_x \left(\frac{h_x}{\sqrt{1 + h_x^2}} \right) \right],$$
(81)

where $\varphi(x,t) = \phi(x,h(x,t),t)$ is the restriction of the velocity potential to the free surface, λ is the surface tension parameter (set to zero in this section), and P is the projection onto zero mean in $L^2(0,2\pi)$. Only h(x,t) and $\varphi(x,t)$ are evolved in time since $\phi(x,y,t)$ can be computed from $\varphi(x,t)$ using (82) below. The velocity components $u=\phi_x, v=\phi_y$ on the free surface are computed from φ as follows. We identify \mathbb{R}^2 with \mathbb{C} and attempt to represent the complex velocity potential $\Phi(z) = \phi(z) + i\psi(z)$ as a Cauchy integral

$$\Phi(z) = \frac{1}{2\pi i} \int_0^{2\pi} \frac{\zeta'(\alpha)}{2} \cot \frac{\zeta(\alpha) - z}{2} \mu(\alpha) d\alpha, \qquad \zeta(\alpha) = \alpha + ih(\alpha), \quad 0 \leqslant \alpha < 2\pi, \tag{82}$$

where $\mu(\alpha)$ is real-valued and we have suppressed t in the notation. Here we used $\alpha = x$ to parametrize the horizontal component of the free surface, but the formulas in this section generalize to allow for mesh refinement or overturning waves if one writes $\zeta(\alpha) = \xi(\alpha) + ih(\alpha)$. The cotangent kernel comes from summing the Cauchy kernel over periodic images

$$\frac{1}{2}\cot\frac{z}{2} = PV\sum_{k \in \mathbb{Z}} \frac{1}{z + 2\pi k}, \qquad (PV = \text{ principal value}).$$
 (83)

Letting z approach $\zeta(\alpha)$ from below and using the Plemelj formula [59] gives

$$\Phi(\zeta(\alpha)^{-}) = -\frac{1}{2}\mu(\alpha) + \frac{i}{2}H\mu(\alpha) + \frac{1}{2\pi i} \int_{0}^{2\pi} K(\alpha,\beta)\mu(\beta) \,d\beta,\tag{84}$$

where

$$K(\alpha, \beta) = \frac{\zeta'(\beta)}{2} \cot \frac{\zeta(\beta) - \zeta(\alpha)}{2} - \frac{1}{2} \cot \frac{\beta - \alpha}{2}.$$
 (85)

The second term of K is included to cancel the singularity of the first term, which makes $K(\alpha, \beta)$ continuous at $\alpha = \beta$, with $K(\alpha, \alpha) = \zeta''(\alpha)/[2\zeta'(\alpha)]$. In fact, the components of K are real analytic, periodic functions of α and β on $\mathbb{R}/2\pi\mathbb{Z}$ if $\zeta(\alpha)$ (i.e. $h(\alpha)$) is real-analytic and periodic. Including this term in $K(\alpha, \beta)$ is accounted for in (84) by the Hilbert transform term, using

$$Hf(\alpha) = \frac{1}{\pi} PV \int_0^{2\pi} \frac{1}{2} \cot \frac{\alpha - \beta}{2} f(\beta) \, d\beta. \tag{86}$$

The real part of (84) gives a second-kind Fredholm integral equation [36] that can be solved for μ given φ ,

$$-\frac{1}{2}\mu(\alpha) + \frac{1}{2\pi} \int_0^{2\pi} \operatorname{Im}\{K(\alpha,\beta)\}\mu(\beta) \, d\beta = \varphi(\alpha), \qquad 0 \le \alpha < 2\pi.$$
 (87)

Differentiating (82), integrating by parts, and using a standard argument for principal value integrals to handle the interchange of α and β in the kernel, one may show [79] that

$$\zeta'(\alpha)\Phi_z(\zeta(\alpha)^-) = -\frac{1}{2}\mu'(\alpha) + \frac{i}{2}H\mu'(\alpha) - \frac{1}{2\pi i}\int_0^{2\pi} K(\beta,\alpha)\mu'(\beta)\,d\beta. \tag{88}$$

Since $\phi_x - i\phi_y = \phi_x + i\psi_x = \Phi_z$, (88) gives an explicit formula for ϕ_x and ϕ_y on the free surface once $\mu(\alpha)$ is known from (87). Equations (87) and (88) are easily discretized with spectral accuracy using the trapezoidal rule on a uniformly spaced grid

$$\alpha_i = 2\pi i/M, \qquad i = 0, \dots, M-1$$
 (89)

to compute integrals, and the Fourier transform to compute derivatives and the Hilbert transform (with symbol $\hat{H}_k = -i \operatorname{sgn}(k)$). For example, (87) becomes

$$-\frac{1}{2}\mu_i + \frac{1}{M} \sum_{j=0}^{M-1} \text{Im}\{K(\alpha_i, \alpha_j)\}\mu_j = \varphi_i, \qquad i = 0, \dots, M-1,$$
 (90)

where we recall that $K(\alpha_i, \alpha_i) = \zeta''(\alpha_i)/[2\zeta'(\alpha_i)]$. We timestep (81) using an 8th order Runge-Kutta method due to Dormand and Prince [39, 69]. We also need h_t in the comparison to the h-model, but this formula is part of the right-hand side of (81).

9.2 Timestepping the h-model

Next we describe an effective method of timestepping the h-model (linear, quadratic or cubic). First, we write it as a first-order system of the form $u_t = Lu + N(u, t)$, which for the cubic case is

$$\underbrace{\frac{\partial}{\partial t} \begin{pmatrix} h \\ h_t \end{pmatrix}}_{u_t} = \underbrace{\begin{pmatrix} 0 & P \\ -g\Lambda & 0 \end{pmatrix} \begin{pmatrix} h \\ h_t \end{pmatrix}}_{Lu} + \underbrace{\begin{pmatrix} P_0(h_t) \\ -\Lambda[(Hh_t)^2] + g\partial_x(hh_x) + g\Lambda(h\Lambda h) + Q(h) \end{pmatrix}}_{N(u,t)}. \tag{91}$$

For the quadratic model, we drop Q(h), and for the linear model, the entire second component of N is set to zero. Here

$$Pf(x) = f(x) - P_0 f, \qquad P_0 f = \frac{1}{2\pi} \int_0^{2\pi} f(x) dx$$
 (92)

are the orthogonal projections onto zero mean, and onto the constant functions, respectively. Though $P_0(h_t)$ is linear, it is convenient to move it from L to N to avoid a Jordan block in the diagonalization of L (see below). To solve the stiff system (91), we use the spectral exponential time differencing scheme of Chen and Wilkening [21], which is an arbitrary-order, fully-implicit variant of the popular fourth-order ETD scheme of Cox and Matthews [29, 48]. To evolve the solution over a timestep, which, for simplicity, we take to be from t = 0 to t = h, we solve the Duhamel integral equation

$$u(t) = e^{Lt}u_0 + \int_0^t e^{(t-\tau)L}N(\tau, u(\tau)) d\tau$$
(93)

by collocation using a Chebyshev-Lobatto grid. In more detail, let

$$t_j = c_j h, \qquad c_j = \frac{1 - \cos(\pi j/\nu)}{2}, \qquad (j = 0, \dots, \nu).$$
 (94)

Given u_0 , we look for u_1, \ldots, u_{ν} such that

$$u_r = e^{t_r L} u_0 + \int_0^{t_r} e^{(t_r - \tau)L} \sum_{j=0}^{\nu} N(t_j, u_j) \ell_j(\tau/h) d\tau, \qquad (r = 1, \dots, \nu),$$
 (95)

where $l_j(s) = \prod_{k \neq j} \frac{s - c_k}{c_j - c_k}$ are the Lagrange polynomials for the Chebyshev-Lobatto grid on [0, 1]. The change of variables $\tau = hs$, $d\tau = hds$ then gives

$$u_r = e^{c_r h L} u_0 + h \sum_{j=0}^{\nu} \left(\int_0^{c_r} e^{(c_r - s)hL} \ell_j(s) \, ds \right) N(c_j h, u_j), \qquad (r = 1, \dots, \nu), \tag{96}$$

which is a nonlinear system of equations that can be solved efficiently using a Newton-Krylov solver; see [21] for details. The algorithm in [21] is designed so the user only has to supply routines to apply U, S and U^{-1} to arbitrary vectors, where $L = USU^{-1}$. Internally, when the Newton-Krylov solver needs to apply $e^{c_r hL}$ and $\int_0^{c_r} e^{(c_r - s)hL} \ell_j(s) ds$ to a sequence of vectors, it does so by asking the user to apply only U, S and U^{-1} . This makes implementing the method on new problems straightforward as long as L can be diagonalized efficiently.

In our case, L is diagonalized by the Fourier transform, as we now explain. Let \mathcal{F} be the "r2c" version of the Fast Fourier Transform, which maps

$$V \ni \begin{pmatrix} u_0 \\ u_1 \\ \vdots \\ u_{M-1} \end{pmatrix} \stackrel{\mathcal{F}}{\longmapsto} \begin{pmatrix} \hat{u}_0 + i\hat{u}_{M/2} \\ \hat{u}_1 \\ \vdots \\ \hat{u}_{M/2-1} \end{pmatrix} \in \hat{V}, \qquad \hat{u}_k = \frac{1}{M} \sum_{j=0}^{M-1} u_j e^{-2\pi i j k/M}. \tag{97}$$

Here we assume M is even, and we note that \hat{u}_0 and $\hat{u}_{M/2}$ are real since $e^{-2\pi i j k/M} \in \{1, -1\}$ when k = 0 or k = M/2. The "missing" Fourier modes are known implicitly from $\hat{u}_{-k} = \overline{\hat{u}_k}$. The mapping \mathcal{F} is an isometry of real vector spaces if we endow V and \hat{V} with the inner products

$$\langle u, v \rangle = \frac{1}{M} \sum_{j=0}^{M-1} u_j v_j, \qquad \langle \hat{u}, \hat{v} \rangle = \hat{u}_0 \hat{v}_0 + \hat{u}_{M/2} \hat{v}_{M/2} + \sum_{k=1}^{M/2-1} 2 \operatorname{Re}\{\overline{\hat{u}_k} \hat{v}_k\}.$$
 (98)

To diagonalize L, we note that both Λ and P in (91) kill constant functions, and we define the finite-dimensional truncations of Λ and P to also kill the Nyquist mode $u_j = (-1)^j$. Thus

$$L = \begin{pmatrix} \mathcal{F}^{-1} & \\ & \mathcal{F}^{-1} \end{pmatrix} \begin{pmatrix} 0 & E \\ -gK & 0 \end{pmatrix} \begin{pmatrix} \mathcal{F} & \\ & \mathcal{F} \end{pmatrix}, \tag{99}$$

where $E = \text{diag}[0, 1, \dots, 1]$, $K = \text{diag}[0, 1, 2, \dots, M/2 - 1]$, and multiplying a vector in \hat{V} by E or K via complex arithmetic is still linear when \hat{V} is regarded as a real vector space. The inner matrix can be diagonalized into 2×2 blocks by a permutation matrix

$$\begin{pmatrix} 0 & E \\ -gK & 0 \end{pmatrix} = \begin{pmatrix} E_e \\ E_o \end{pmatrix} \begin{pmatrix} A_0 \\ & \ddots \\ & & A_{M/2-1} \end{pmatrix} \begin{pmatrix} E_e^T & E_o^T \end{pmatrix}, \qquad A_0 = \begin{pmatrix} 0 & 0 \\ 0 & 0 \end{pmatrix}, \qquad (100)$$

where $E_{e,ij} = \delta_{2i,j}$, $E_{o,ij} = \delta_{2i+1,j}$ for $0 \le i < M/2$, $0 \le j < M$. Left-multiplication by E_e or E_o selects the even-index or odd-index rows, respectively; right-multiplication by E_e^T or E_o^T selects even or odd-index columns; and applying (E_e^T, E_o^T) to $[\hat{h}; \hat{h}_t]$ interlaces the components of $\hat{h} \in \hat{V}$ and $\hat{h}_t \in \hat{V}$, so that $\partial_t \hat{h}_k$ follows \hat{h}_k . Finally, A_0 is already diagonal while $A_k = Q_k S_k Q_k^{-1}$ with

$$Q_k = \begin{pmatrix} 1 & 1 \\ i\sqrt{gk} & -i\sqrt{gk} \end{pmatrix}, \quad S_k = \begin{pmatrix} i\sqrt{gk} \\ -i\sqrt{gk} \end{pmatrix}, \quad Q_k^{-1} = \frac{1}{2} \begin{pmatrix} 1 & -i/\sqrt{gk} \\ 1 & i/\sqrt{gk} \end{pmatrix}. \quad (101)$$

The complex numbers in E, K, E_e , E_o , A_k , Q_k , Q_k^{-1} and S_k actually represent real 2×2 matrices with the identification

$$\alpha + i\beta \longleftrightarrow \begin{pmatrix} \alpha & -\beta \\ \beta & \alpha \end{pmatrix}$$
. Example: $S_k = \begin{pmatrix} 0 & -\sqrt{gk} \\ \sqrt{gk} & 0 \\ & 0 & \sqrt{gk} \\ & -\sqrt{gk} & 0 \end{pmatrix}$. (102)

Treating the entries of \hat{V} as complex numbers rather than flattening \hat{V} to \mathbb{R}^M by interlacing real and imaginary parts is convenient, but gets confusing in the last step when complex eigenvalues arise. The final step of diagonalizing L (had we flattened \hat{V}) would be to diagonalize the real matrix S_k in (102), which would lead to a pair of double eigenvalues $\pm i\sqrt{gk}$. But applying any power series to S_k in (101) and then flattening will give the same result as applying the power series directly to S_k in (102). In particular, $e^{c_r h S_k}$ and

 $e^{(c_r-s)hS_k}$, which are needed to compute e^{c_rhL} and $e^{(c_r-s)hL}$ in (96), can be computed either way. This justifies not flattening \hat{V} , and cuts the number of eigenvalues that are explicitly dealt with in half — each double-eigenvalue in (102) appears only once in (101).

Note that moving $P_0(h_t)$ over to N(u,t) in (91) was necessary to avoid a Jordan block in A_0 in (100). We also remark that normally one wants to include the highest-order differential operators in L, but in our case they are nonlinear and depend on time, so this was not possible. However, the method still does not suffer from severe CFL constraints since fully implicit Runge-Kutta schemes based on Lobatto quadrature are L-stable [39]. The above method reduces to such a scheme when L=0, and we would not expect instabilities to arise by separating the linear part of the operator into a Duhamel-based formulation.

9.3 Comparison of water waves and the h-model

As a first test, we consider the family of solutions $h(x,t) = \epsilon \tilde{h}(x,t)$, $\varphi(x,t) = \epsilon \tilde{\varphi}(x,t)$ with

Example 1:
$$\widetilde{h}(x,0) = \frac{1}{5}\sin x + \frac{1}{10}\sin(2x) + \frac{1}{5}\sin(3x), \qquad \widetilde{\varphi}(x,0) = 0.$$
 (103)

The maximum slope of the initial wave profile h(x,0) occurs at the origin, and is equal to ϵ . The wave starts at rest and evolves under the influence of gravity. The solution of the full Euler equations for $\epsilon = 5/3$ for $0 \le t \le 0.625$ is shown in Figure 1(a), along with the spatial Fourier mode amplitudes (panel b) of h(x,t) at the times shown in panel (a). Only positive index Fourier modes are shows since $c_{-k} = \overline{c_k}$. A 3072-point spatial grid was used, with 720 uniform timesteps of the DOPRI8 Runge-Kutta method [39, 69]. Every 18th step was recorded (at t = k/64, $0 \le k \le 40$). At t = 0.625 = 40/64, a jet begins to form in each of the troughs, with the lowest trough containing the strongest jet.

Panels (c) and (d) of Figure 1 compare the solutions of the linear, quadratic and cubic h-models with that of the full Euler equations with $\epsilon = 5/6$ in (103) at $t \in \{0, \frac{1}{2}T, \frac{3}{4}T, T\}$, where T = 40/64. At this amplitude, both the linear and quadratic models miss the bulge in the lowest trough as the jet begins to form, whereas the cubic model captures it closely. If ϵ is doubled to $\epsilon = 5/3$ (as in panel a), niether the cubic nor quadratic models can be evolved all the way to t = 40/64. Panel (e) of Figure 1 shows that the quadratic model (on a 3072-point grid) appears to form a corner singularity around t = 37/64, and is far from the corresponding Euler solution at this time. For the cubic model (evolved on a 1024-point grid), high-frequency Fourier modes begin to grow at t = 12/64. By t = 30/64, roundoff errors in these high-frequency modes have been amplified to be comparable in size to the leading modes. The solution completely blows up shortly afterwards, with values on the grid jumping from O(1) at 30/64 to $O(10^{250})$ at 31/64. Increasing the number of timesteps by a factor of 1000 did not change the time at which the instability begins or the growth rate of the modes, so this is not likely a CFL issue. However, increasing the spatial grid size does affect the blow-up time since higher-frequency modes grow faster. We omit a figure showing this for Example 1 as similar behavior is observed in Example 3 below. Panel (f) of Figure 1 shows the L^2 error of the linear, quadratic and cubic models at t = 40/64 versus ϵ , where the L^2 errors have been scaled by ϵ^{-1} to account for the decreasing norm of the exact solution As expected, these errors decay as $O(\epsilon^k)$, where k=1 for the linear h-model, k=2 for the quadratic h-model, and k = 3 for the cubic h-model.

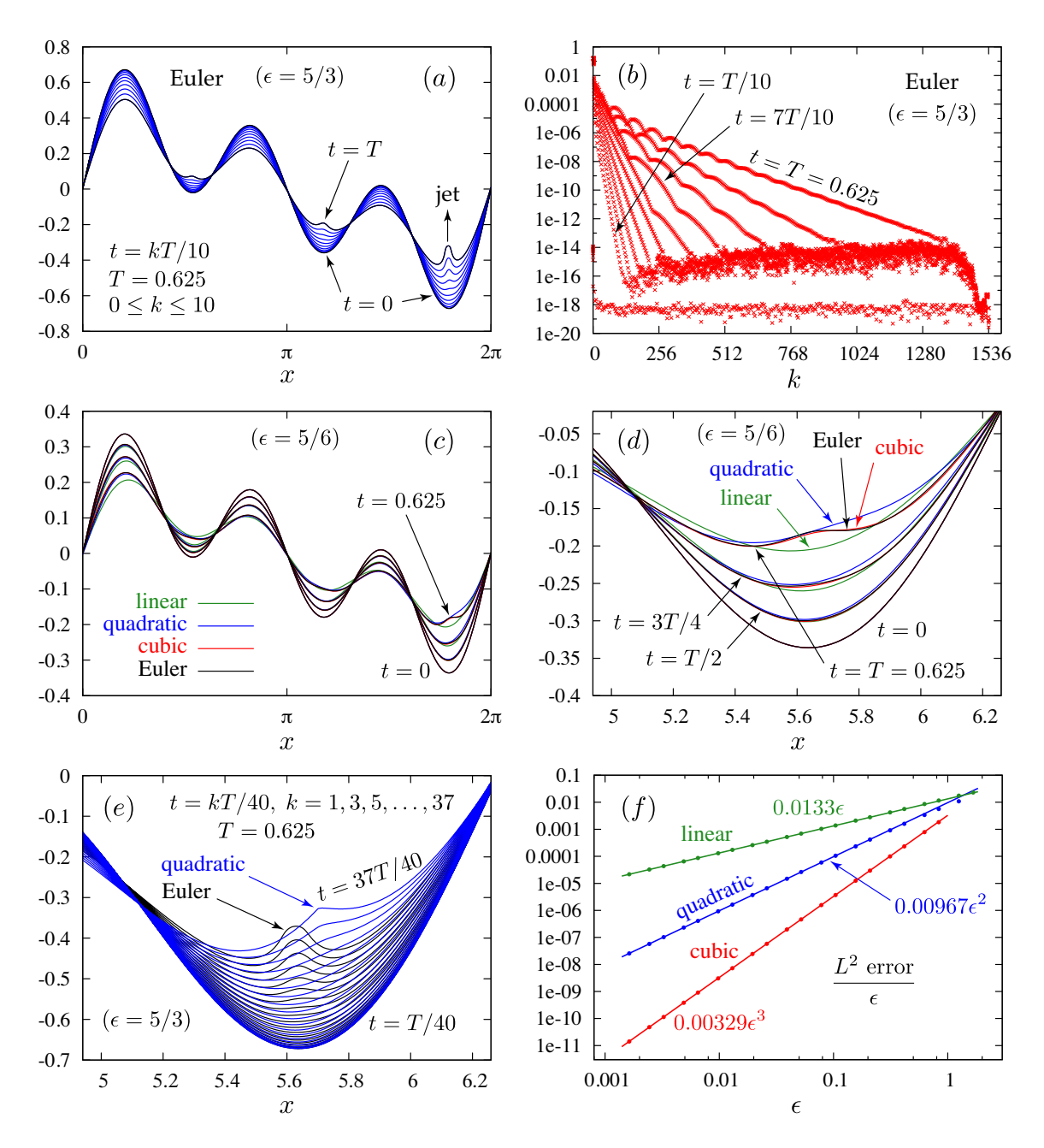


Figure 1: Comparison of the linear, quadratic and cubic h-models to the full Euler equations for Example 1. (a) Large-amplitude Euler solution with $\epsilon = 5/3$. (b) Amplitude of Fourier modes for this solution. (c and d) The cubic model remains close to the true solution for $\epsilon = 5/6$ and $0 \le t \le 0.625$, whereas the linear and quadratic models miss key features. (e) The quadratic model forms a corner in the $\epsilon = 5/3$ case. (f) Relative L^2 -errors versus ϵ .

The second example we consider consists of an initial bulge over a flat surface evolving from rest. More specifically, we consider the family of functions

Example 2:
$$\tilde{h}_n(x,0) = \frac{2}{n} \left(1 + \frac{1}{n^2} \right)^{\frac{n^2 - 1}{2}} \left[\sin^{n^2 + 1} \frac{x}{2} - \frac{\Gamma((n^2/2) + 1)}{\sqrt{\pi} \Gamma((n^2/2) + (3/2))} \right], \quad (104)$$

where $n \in \{1, 3, 5, 7, ...\}$. The constants were chosen so that $\tilde{h}_n(x, 0)$ has zero mean and maximum slope ± 1 , occuring where $\tan(x/2) = \pm n$. The cases n = 7 and n = 25 are shown in panel (a) of Figure 2. Panel (b) shows that the L^2 error at t = 6, scaled by ϵ^{-1} , decays at the expected order as $\epsilon \to 0$ for n = 7 and n = 25. For n = 7, the best-fit lines shown are 0.0326ϵ , $0.0156\epsilon^2$ and $0.00476\epsilon^3$. For n = 25, they are 0.00542ϵ , $0.00337\epsilon^2$ and $0.000524\epsilon^3$, which are smaller than in the n = 7 case. This is not surprising as the L^2 -norm of the underlying wave is also smaller when n = 25.

Panels (c,d,e) of Figure 2 compare solutions of the Euler equations with those of the linear, quadratic and cubic h-models with $\epsilon = 0.429$ and n = 25 over $0 \le t \le 1$ (panel c), $1 \le t \le 2$ (panel d), and $5 \le t \le 6$ (panel e). The linear model already deviates substantially from the exact solution by t = 0.4 (panel c), when the initial bulge is still accelerating downward. The quadratic and cubic models remain close to the Euler solution throughout the evolution to t = 6 (panel e), correctly damping out the wave near the origin and propagating the correct number of ripplies outward in both directions. The quadratic model develops a sharper crest at t = 1 (panel d) than the Euler solution, which also sharpens somewhat at this time. For both equations, the wave becomes smoother again. This can be seen in panel (f), where the Fourier mode amplitudes decay more slowly at t=1 than at t=0 or t=6. The minimum decay rate for both equations happens near t=1. The quadratic model has roughly 6 times as many active modes as the Euler solution at t=1 due to the excessive sharpening at the crest observed in panel (d). At later times (e.g. panel e), the quadratic model retains remnants of the overly sharp crest that formed at t=1, with smaller-scale features visibly deviating from the exact solution (though the overall wave profiles are similar.) The cubic model is nearly indistinguishable from the Euler model at the resolution of the graphs in panels (d) and (e). It has about twice as many active Fourier modes as the Euler solution at t=1 and t=6, as shown in panel (q). The Euler modes are the same in panels (f) and (g), and all three equations have the same Fourier coefficients at t=0 in these plots.

Our third example consists of a family of standing water waves computed using the overdetermined shooting method described in [78, 79]. Unlike the previous two examples, the waves in this family are not related by a simple scaling of the initial condition via $h(x,0) = \epsilon \tilde{h}(x,0)$, $\varphi(x,t) = \epsilon \tilde{\varphi}(x,t)$. In the previous examples, we chose $\tilde{h}(x,0)$ to have maximum slope 1 so that ϵ was the maximum slope of h(x,0). For standing waves, we match this latter property:

Example 3 (standing waves):
$$\epsilon = \text{maximum slope of } h(x, 0).$$
 (105)

Here we assume the fluid is initially at rest. As before, we choose the length-scale so that the spatial period is 2π after non-dimensionalization. Let T (which depends on ϵ) be half the temporal period of the standing wave so that the wave comes to rest when $t \in T\mathbb{Z}$. At even

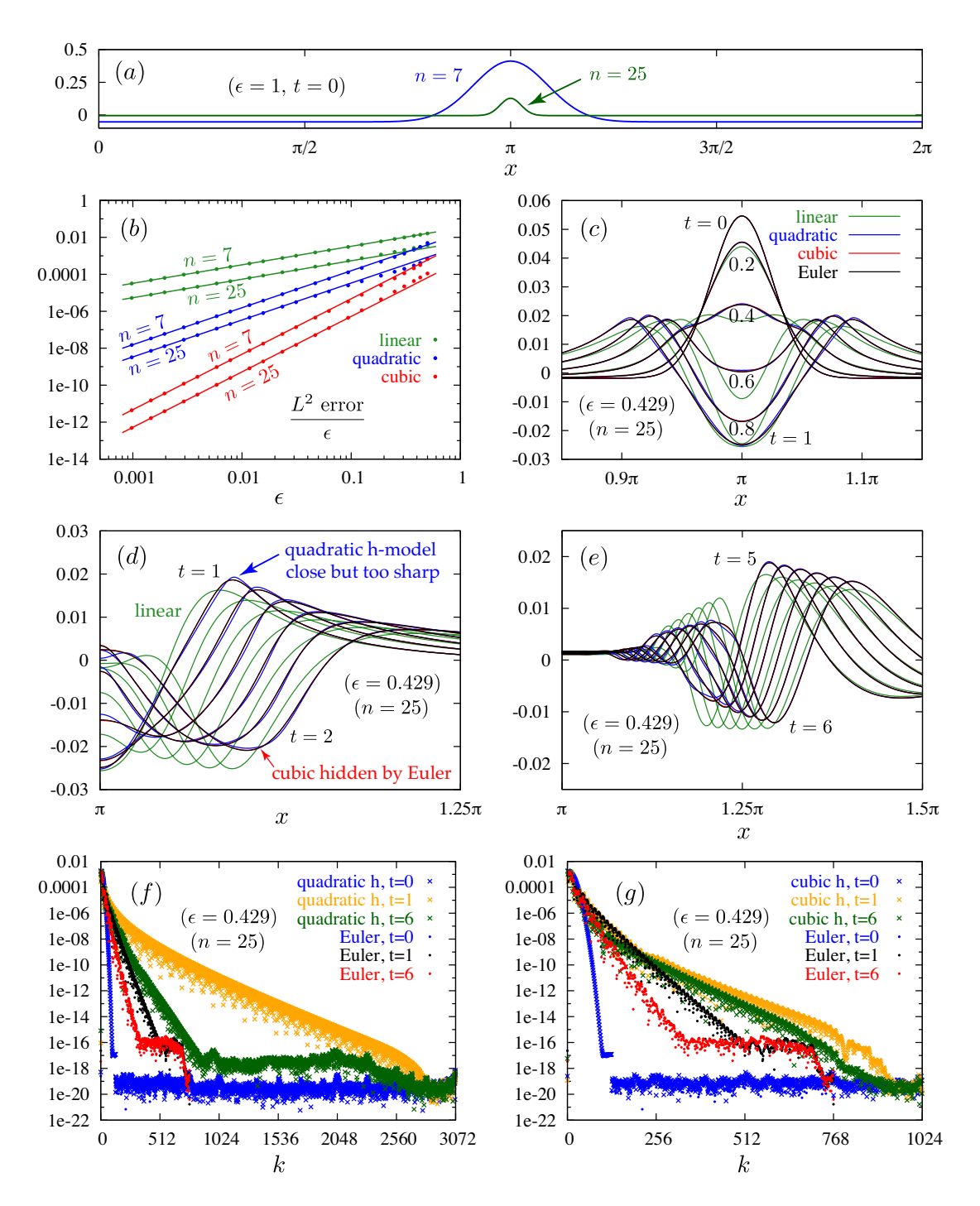


Figure 2: Comparison of the linear, quadratic and cubic h-models to the full Euler equations for Example 2. (a) Initial wave profiles before scaling by ϵ . (b) Relative L^2 -errors versus ϵ . (c, d, e) Solutions with n=25 and $\epsilon=0.429$ at the times shown. (f, g) Comparison of Fourier mode amplitudes at t=0,1,6. The sharper wave crest in the solution of the quadratic model at t=1 leads to slower mode decay than the Euler or cubic solutions.

multiples of T, the wave crests are assumed to be located at $x \in 2\pi\mathbb{Z}$, and at odd multiples they are located at $x \in (\pi + 2\pi\mathbb{Z})$.

Characterizing the amplitude of the wave by its maximum slope is useful for comparing with Examples 1 and 2, but it is not the most convenient for actually computing standing waves. In the numerical algorithm of Wilkening and Yu[79], a Fourier coefficient of the initial condition was used as the bifurcation parameter. For low-amplitude waves, the initial amplitude of the fundamental mode is a natural choice. Yet another choice is half the maximum crest to trough height $(\frac{1}{2}H_{CT})$. In all three cases (slope, mode amplitude, or $\frac{1}{2}H_{CT}$), assuming g = 1,

$$h(x,t) = \epsilon \cos x \cos t + O(\epsilon^2). \tag{106}$$

Building on previous work [70, 68, 77], Schwartz and Whitney [72] developed a recursive algorithm to compute the power series expansion for standing water waves of this type in conformal variables, and computed the first 25 terms. Their choice of amplitude was $\frac{1}{2}H_{CT}$, which we denote by ε . While the full representation of the wave profile and velocity potential is too complicated to reproduce here, we can report the leading terms of the period and maximum slope:

$$\frac{T}{\pi} = 1 + \frac{1}{2}\varepsilon^2 - \frac{7}{256}\varepsilon^4 + O(\varepsilon^6), \qquad \epsilon = \varepsilon + \frac{1}{2}\varepsilon^3 + O(\varepsilon^5). \tag{107}$$

Amick and Toland proved that the terms in the Schwartz/Whitney expansion are uniquely determined to all orders [13], but the question of whether the series has a positive radius of convergence remains open. Recent work using Nash-Moser theory has been able to establish existence on a Cantor set of the bifurcation parameter close to zero-amplitude [47]. Regardless of the eventual convergence or divergence of the series, truncating the series yields a family of initial conditions (over a range $0 \le \varepsilon \le \varepsilon_{\text{max}} \approx 0.06$ when 25 terms are retained) that return to their starting configurations to within machine precision when evolved under the Euler equations. The shooting method in [79] gives solutions that agree with the Schwartz and Whitney series to all 16 digits at small amplitude, but is not limited to such a narrow range of ε to find solutions that are time-periodic to machine precision.

For each standing wave computed by the shooting method, we find the maximum slope via Newton's method to determine ϵ . We then evolve the h-models using the initial conditions of the standing wave and compare them to the Euler solution at t=T. Panel (a) of Figure 3 shows that the relative errors in the linear, quadratic and cubic models decay at the expected rates. Panel (b) shows snapshots of the solutions of the h-models and the Euler equations for the $\epsilon=0.498$ wave at $t=\frac{1}{4}T, \frac{1}{2}T, \frac{3}{4}T$ and t=T. This choice of ϵ was the largest (among the waves we computed) in which the solution of the quadratic h-model remains regular for $0 \le t \le T$. We see in panel (b) that the quadratic model nearly forms a corner at t=T, which also leads to slow decay of its Fourier modes in panel (c) as t approaches t. The Euler solution returns to a spatial phase shift (by t) of its initial condition to 14 digits. Its Fourier modes decay to t0 to t1 by t2 grid points in the computation. We also used 192 grid points to evolve the cubic model. The solution remains well-resolved in Fourier space over this time (panel d), and remains nearly indistinguishable from the Euler solution at the resolution of panel (b) over t2 to t3. We also note in panel (b) that the solution of the quadratic model remains close to the Euler solution until t3. We the linear model

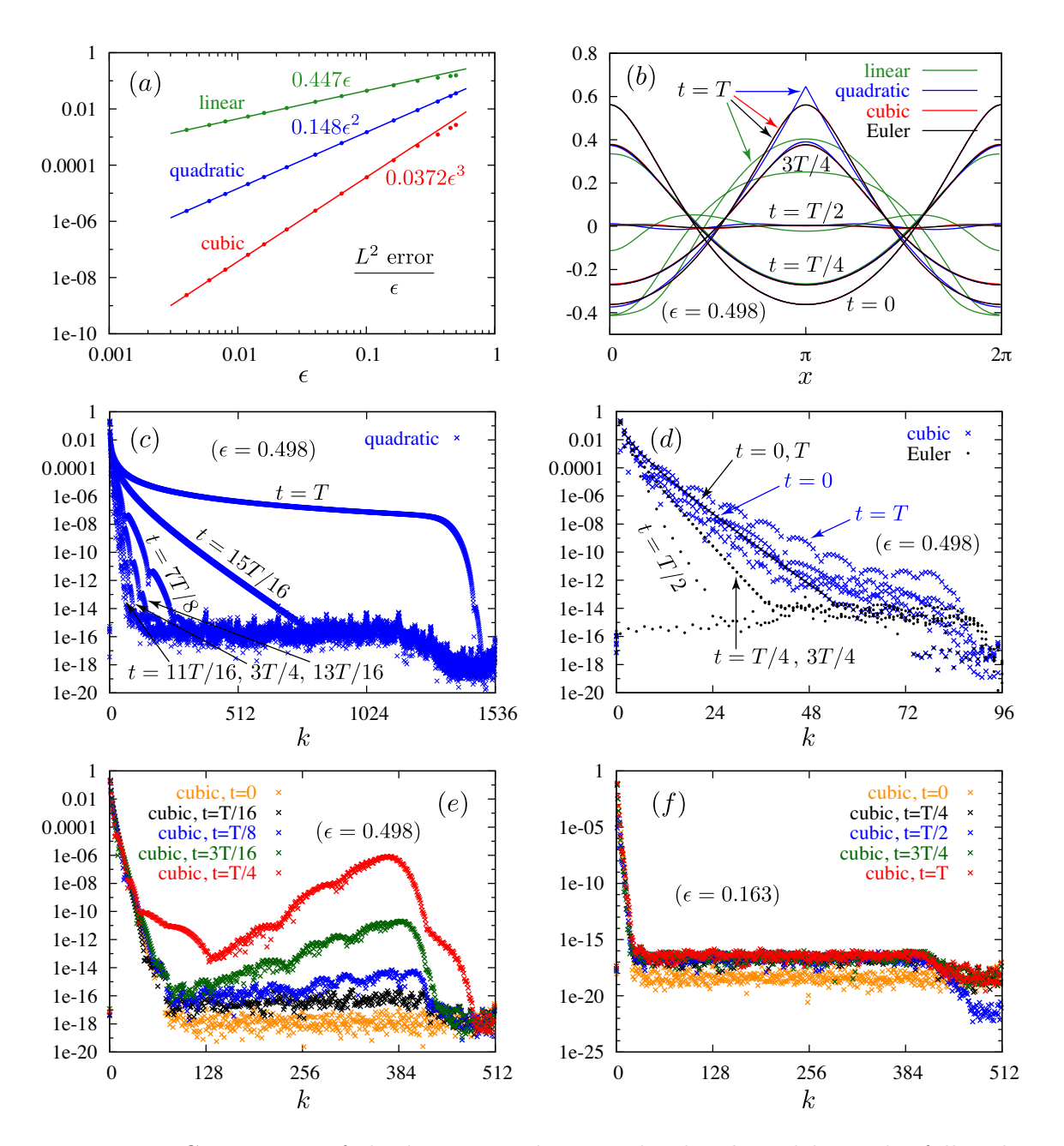


Figure 3: Comparison of the linear, quadratic and cubic h-models to the full Euler equations for Example 3. (a) Relative L^2 -errors versus ϵ . (b) Snapshots of the solutions at t = 0, T/4, T/2, 3T/4, T for $\epsilon = 0.498$. The quadratic model nearly forms a corner at t = T. (c) The formation of a corner causes high-frequency Fourier mode amplitudes to grow as $t \to T$ in the quadratic model. (d) The cubic model and Euler equations remain well-resoved with 192 Fourier modes. (Only 96 are shown since $c_{-k} = \overline{c_k}$.) (e, f) Over short times or small amplitude, the cubic model remains well-posed; however, for $\epsilon = 0.498$, with 1024 modes, the cubic model loses stability for t > T/16. The solution completely blows up shortly after t = T/4.

already deviates substantially near x = 0 and $x = 2\pi$ at t = T/4. It remains accurate in the trough at least until t = T/4, but is completely wrong throughout the domain by t = T/2.

At this large amplitude ($\epsilon = 0.498$), the cubic model relies on Fourier truncation to remain well-posed. In panel (e) of Figure 3, we increase the number of gridpoints from 192 to 1024 with the same initial data as in panel (d), and find that high-frequency modes begin to grow rapidly shortly after t = T/16. This picture is independent of the number of timesteps taken — increasing the number of timesteps by a factor of 1000 led to a similar picture (not shown), except that applying the filter 1000 times as often led to slight suppression of the mode amplitudes in the range $300 \le k \le 512$. Thus, around t = T/16, the solution of the cubic model appears to evolve to a state where the PDE ceases to be well-posed. By contrast, the solution of the quadratic model does not show signs of instability regardless of the grid size until t = T — the growth in mode amplitudes in panel (c) is due to formation of a geometric singularity rather than ill-posedness. In panel (f), we see that the cubic model remains well-posed over the whole interval $0 \le t \le T$ for a smaller amplitude wave ($\epsilon = 0.163$). Here again we used 1024 gridpoints, even though 48 would have been sufficient to fully resolve the solution spectrally. We observed similar behavior in Examples 1 and 2, where large-amplitude waves were found to form corners at their crests in the quadratic model, and caused the solution to leave the realm of well-posedness for the cubic model. (The sharpening feature in Figure 2d for the quadratic model forms a corner at larger amplitude).

In Figure 4, we return to the solution of the full Euler equations for Example 1 with $\epsilon =$ 5/3. Here we switch to an angle-arclength parametrization of the free surface [41, 42, 43, 11], which allows for overturning waves. We continue to define T = 0.625 and evolve to t = 1.9T. Panel (a) shows that the jets that were beginning to form in the troughs at t = T grow in height to become the tallest points on the free surface at t=1.9T. The jet from the lowest trough overtakes that of the middle trough around t = 1.4562T, and is on track to overtake that of the highest trough around t = 1.9451T, where we extrapolated from the last 4 timesteps. Panel (b) shows a close-up of the jet from the lowest trough, which widens and flattens out as it decelerates, causing the wave to overturn on both sides of the jet. The overturn times are t = 1.335T on the left and 1.343T on the right. Panel (c) shows the aplitude of the Fourier modes as the solution evolves. The grid was refined 6 times, from 1024 gridpoints at the beginning to 16384 at the end. Roundoff errors become larger as the grid is refined due to increased cancellation in the formula (85) for $K(\alpha, \beta)$. Each grid refinement also leads to some growth in high-frequency modes that were being suppressed by the filter on the coarser mesh and suddenly are not. (We use the 36th order filter of Hou and Li [40]).

Once the wave overturns, there are 3 possible outcomes. It could return to being single-valued, which sometimes happens after a vortex sheet with surface tension overturns [10, 11], but seems unlikely here as there is no physical mechanism to slow down the overturning wave. It could self-intersect in a splash singularity [19, 27]. Or it could form a corner at the tip of the overturning wave, similar to the way the quadratic h-model tends to form singularities. This would coincide with dP/dn approaching zero at the corner, so that the Rayleigh-Taylor condition dP/dn < 0 ceases to hold. Panels (d, e) of Figure 3 show dP/dn plotted parametrically versus x at various times. We see that indeed, dP/dn appears to be increasing to 0 at the tip of each overturning wave. However, computing dP/dn involves

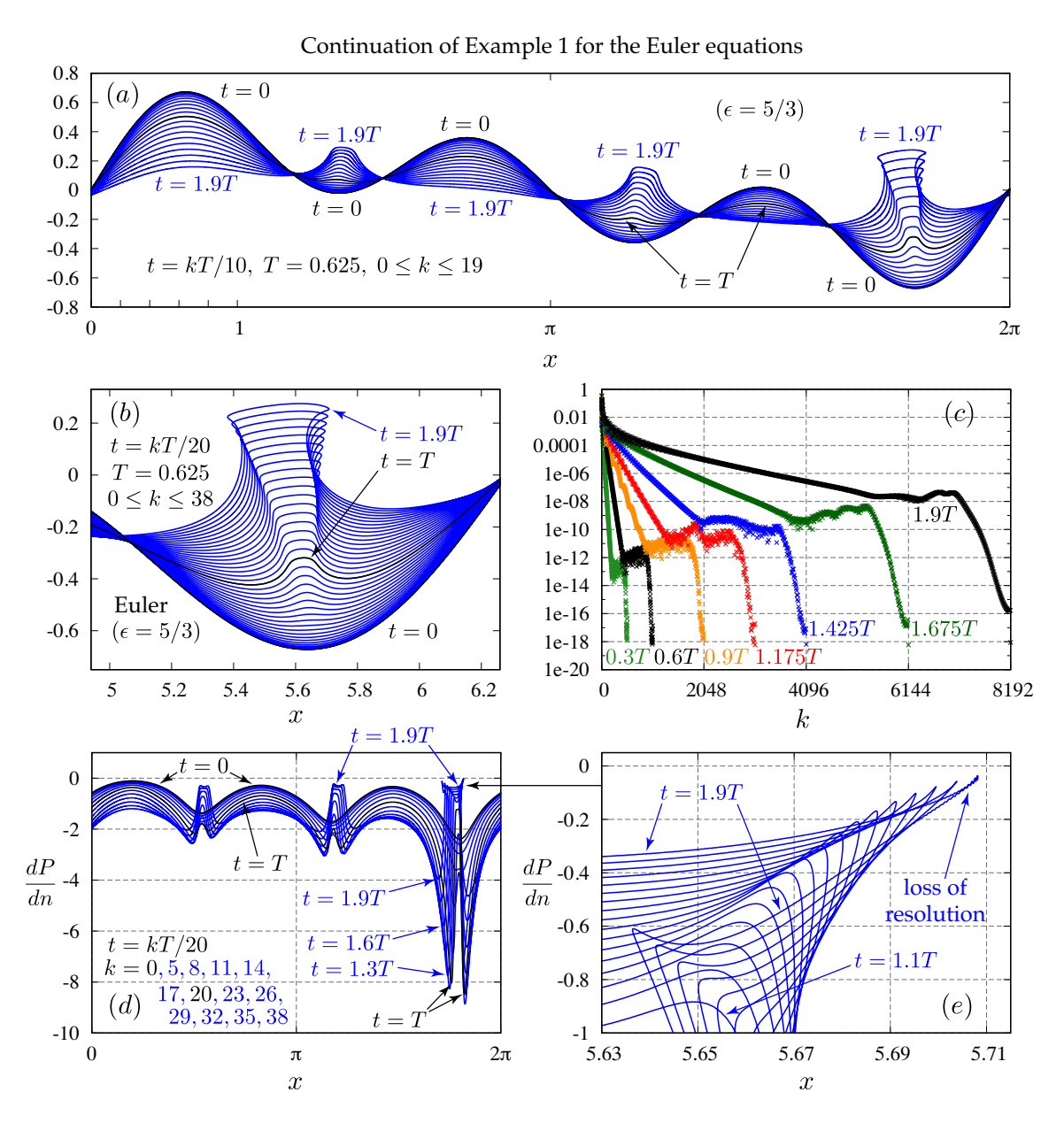


Figure 4: (a) Evolution of the $\epsilon=5/3$ wave with initial condition (103) to t=1.9T, where T=0.625 is the final time in Figure 1. The aspect ratio is 1:1. (b) A closer look at the jet forming in the lowest trough, which overturns on the left around t=1.335T and on the right around t=1.343T. (c) Amplitude of the Fourier modes at the times shown. The spatial grid was refined 6 times in the course of the evolution. (d,e) The normal derivative of pressure versus x as time evolves. The computed value of dP/dn runs out of precision but approaches zero near the tip of the overturning wave at t=1.9T, indicating corner formation.

taking a derivative of the solution, and we were not able to maintain enough digits of accuracy in double-precision to definitively say that dP/dn reaches zero. The Rayleigh-Taylor condition plays a key role in the local well-posedness of the water wave problem in the absence of surface tension (see the references given in the introduction). Further investigation will be pursued in future work, where we will provide details of the method for tracking overturning waves and computing dP/dn. Our main point in this example is to show that the type of breakdown we observe in the quadratic h-model, where the solution forms a geometric singularity, may occur in the Euler equations as well.

9.4 Conclusions from our numerical results

We have shown that the quadratic and cubic h-models can be solved efficiently using a Fourier representation in space and an exponential time differencing scheme in time. Comparing the results to the solution of the full water wave equations on three test problems, we find that the quadratic and cubic h-models capture features of the solution that are completely missed by linear theory, such as sharpening crests and jet formation. We confirm that the linear, quadratic and cubic h-models converge to the exact solution at the expected rates as $\epsilon \to 0$, and explore how each model breaks down at very large amplitude. The linear model does not form singularities since each mode of the initial condition evolves independently. For large-amplitude initial conditions, the quadratic model appears to form sharp corners at wave crests in finite time while the cubic model appears to evolve to an unstable state in finite time after which the growth rate of Fourier modes increases without bound as the mode index increases. In one of the examples, the full water wave appears to form a corner singularity in finite time, with dP/dn approaching zero at a sharpening wave crest that forms after the wave has overturned.

Acknowledgements

We thank the anonymous referees for their numerous suggestions that have improved the exposition of this article. JW was supported by NSF DMS-1716560 and by the Department of Energy, Office of Science, Applied Scientific Computing Research, under award number DE-AC02-05CH11231. RGB was partially funded by University of Cantabria and the Department of Mathematics, Statistics and Computation. SS was supported by NSF DMS-1301380, the Department of Energy, Advanced Simulation and Computing (ASC) Program, and by DTRA HDTRA11810022.

A Basic commutator identities

In deriving the cubic h-model, we make use of the following identities:

$$\begin{split} &\Lambda\big[(H\partial_t h)\Lambda\big(\llbracket h,H\rrbracket\partial_t h\big)\big]-\Lambda\big[(H\partial_t h)(\partial_1 h)(\partial_t h)\big]=\Lambda\big[(H\partial_t h)\Lambda\big(hH\partial_t h\big)\big]+\Lambda\big[(H\partial_t h)h(\partial_1 \partial_t h)\big]\,,\\ -\partial_1\big(\llbracket \partial_t h,H\rrbracket\partial_1\big(\llbracket h,H\rrbracket\partial_t h\big)\big)-\partial_1\big(\llbracket \partial_t h,H\rrbracket\Lambda(h\partial_t h)\big)&=-\partial_1\big(\llbracket \partial_t h,H\rrbracket\partial_1\big(hH\partial_t h\big)\big)\,,\\ &\partial_1\big(\llbracket h,H\rrbracket\partial_1(\partial_t hH\partial_t h)\big)-\partial_1\big[\llbracket h,H\rrbracket\Lambda(\partial_t h)^2\big]&=\partial_1\big(\llbracket h,H\rrbracket\partial_1(\llbracket \partial_t h,H\rrbracket\partial_t h)\big)\,,\\ -H\big[(\partial_1 h)h\partial_1^2 h\big]+\frac{1}{2}\partial_1\big[h^2(\Lambda\partial_1 h)\big]-\frac{1}{2}H(h^2\partial_1^3 h)&=\frac{1}{2}\partial_1\llbracket h^2,H\rrbracket\partial_1^2 h, \end{split}$$

and

$$H[(\partial_{1}\partial_{t}h)\partial_{1}(hH\partial_{t}h)] + H[(\partial_{1}h)\partial_{1}((\partial_{t}h)(H\partial_{t}h))] - 2H[(\partial_{1}h)(\partial_{1}\partial_{t}h)(H\partial_{t}h)]$$

$$+ H[h(\partial_{t}h)\partial_{1}\Lambda\partial_{t}h]$$

$$= H[(\partial_{1}\partial_{t}h)(\partial_{1}h)(H\partial_{t}h)] + H[h(\partial_{1}\partial_{t}h)(\Lambda\partial_{t}h)] + H[(\partial_{1}h)(\partial_{1}\partial_{t}h)(H\partial_{t}h)]$$

$$+ H[(\partial_{1}h)(\partial_{t}h)(\Lambda\partial_{t}h)] - 2H[(\partial_{1}h)(\partial_{1}\partial_{t}h)(H\partial_{t}h)] + H[h(\partial_{t}h)\partial_{1}\Lambda\partial_{t}h]$$

$$= H[\partial_{1}((h\partial_{t}h)(\Lambda\partial_{t}h))]$$

$$= \Lambda[(h\partial_{t}h)(\Lambda\partial_{t}h)].$$

B Another proof of Theorem 3

Proof of Theorem 3. The solution as a series. Using the ansatz (25), the quadratic h-model (51) can be written as

$$\partial_t^2 \widetilde{h} = -g\Lambda \widetilde{h} - \epsilon \Lambda (H \partial_t \widetilde{h})^2 + g\epsilon \left(\partial_1 (\widetilde{h} \partial_1 \widetilde{h}) + \Lambda (\widetilde{h} \Lambda \widetilde{h}) \right), \tag{108}$$

with initial conditions (28). We expand \tilde{h} as in (26) for functions $h_k : \mathbb{S}^1 \to \mathbb{R}$ to be determined. Substituting into (108) we find that

$$\partial_t^2 h_k = -g\Lambda h_k + \sum_{j=0}^{k-1} \left[\Lambda(gh_j \Lambda h_{k-1-j} - H\partial_t h_j H\partial_t h_{k-1-j}) + g\partial_1(h_j \partial_1 h_{k-1-j}) \right]$$
(109)

with initial conditions

$$h_0(x_1, 0) = \frac{h_{\text{init}}(x_1)}{\epsilon}, \ \partial_t h_0(x_1, 0) = \frac{\dot{h}_{\text{init}}(x_1)}{\epsilon}, h_k(x_1, 0) = \partial_t h_k(x_1, 0) = 0 \ k \geqslant 1.$$
 (110)

Using the Fourier series expansion, (109) shows that each Fourier component satisfies the differential equation

$$\partial_t^2 \hat{h}_k(\ell, t) = -g|\ell| \hat{h}_k(\ell, t) + f(\ell, t), \qquad (111)$$

where f is given by

$$f(\ell,t) = \sum_{j=0}^{k-1} \sum_{m=-\infty}^{\infty} \left[-|\ell| \left((-i \operatorname{sgn}(\ell-m)) \, \hat{\partial}_t \hat{h}_j(\ell-m,t) \, (-i \operatorname{sgn}(m)) \, \hat{\partial}_t \hat{h}_{k-1-j}(m,t) \right) + g \left(i \ell \hat{h}_j(\ell-m,t) i m \hat{h}_{k-1-j}(m,t) + |\ell| \hat{h}_j(\ell-m,t) |m| \hat{h}_{k-1-j}(m,t) \right) \right].$$
(112)

We note that integration of (109) shows that

$$\int_{\mathbb{S}^1} h_k(x_1, t) = 0 \text{ and } \int_{\mathbb{S}^1} \partial_t h_k(x_1, t) ds = 0 \,\forall \, t \geqslant 0.$$
 (113)

Solving the ODE (111) for k = 0, we find that

$$\hat{h}_0(\ell, t) = \hat{h}_0(\ell, 0) \cos\left(\sqrt{g|\ell|}t\right) + \frac{\hat{c}_t \hat{h}_0(\ell, 0)}{\sqrt{g|\ell|}} \sin\left(\sqrt{g|\ell|}t\right).$$

Similarly, the solution to (111) for k > 0 is

$$\begin{split} \widehat{h}_k(\ell,t) &= -\frac{\cos\sqrt{g|\ell|}t}{\sqrt{g|\ell|}} \int_0^t f(s) \sin\left(\sqrt{g|\ell|}s\right) \, ds + \frac{\sin\sqrt{g|\ell|}t}{\sqrt{g|\ell|}} \int_0^t f(s) \cos\left(\sqrt{g|\ell|}s\right) \, ds \\ &= \frac{1}{\sqrt{g|\ell|}} \int_0^t f(s) \sin\left(\sqrt{g|\ell|}(t-s)\right) \, ds \,, \end{split}$$

and hence

$$\partial_t \hat{h}_k(\ell, t) = \int_0^t f(s) \cos\left(\sqrt{g|\ell|}(t - s)\right) ds.$$
 (114)

Using the expression (112), we have that for $k \ge 1$, \hat{h}_k and $\partial_t \hat{h}_k$ verify the following recursion relations:

$$\hat{h}_{k}(\ell,t) = \frac{1}{\sqrt{g|\ell|}} \int_{0}^{t} \left[-\sum_{j=0}^{k-1} \sum_{m=-\infty}^{\infty} |\ell| \left((-i\operatorname{sgn}(\ell-m)) \,\partial_{t} \hat{h}_{j}(\ell-m,s) \,(-i\operatorname{sgn}(m)) \,\partial_{t} \hat{h}_{k-1-j}(m,s) \right) \right. \\
+ g \sum_{j=0}^{k-1} \sum_{m=-\infty}^{\infty} i\ell \hat{h}_{j}(\ell-m,s) im \hat{h}_{k-1-j}(m,s) \\
+ g \sum_{j=0}^{k-1} \sum_{m=-\infty}^{\infty} |\ell| \hat{h}_{j}(\ell-m,s) |m| \hat{h}_{k-1-j}(m,s) \right] \sin \left(\sqrt{g|\ell|} (t-s) \right) ds, \quad (115)$$

and

$$\partial_{t}\widehat{h}_{k}(\ell,t) = \int_{0}^{t} \left[-\sum_{j=0}^{k-1} \sum_{m=-\infty}^{\infty} |\ell| \left((-i\mathrm{sgn}(\ell-m)) \,\partial_{t}\widehat{h}_{j}(\ell-m,s) \,(-i\mathrm{sgn}(m)) \,\partial_{t}\widehat{h}_{k-1-j}(m,s) \right) \right. \\
\left. + g \sum_{j=0}^{k-1} \sum_{m=-\infty}^{\infty} i\ell \widehat{h}_{j}(\ell-m,s) im \widehat{h}_{k-1-j}(m,s) \right. \\
\left. + g \sum_{j=0}^{k-1} \sum_{m=-\infty}^{\infty} |\ell| \widehat{h}_{j}(\ell-m,s) |m| \widehat{h}_{k-1-j}(m,s) \right] \cos \left(\sqrt{g|\ell|}(t-s) \right) ds . \tag{116}$$

Existence. We fix $1 \ll R \in \mathbb{Z}^+$. Given $\epsilon > 0$, we seek solutions h of (51) having the form

$$h(x_1, t) = \sum_{k=0}^{\infty} \epsilon^{k+1} h_k(x_1, t) \text{ and } \partial_t h(x_1, t) = \sum_{k=0}^{\infty} \epsilon^{k+1} \partial_t h_k(x_1, t).$$
 (117)

The series in (117) are respectively bounded by

$$\sup_{0 \le t \le T} \sum_{k=0}^{\infty} \epsilon^{k+1} \|h_k(t)\|_{X_1} \text{ and } \sup_{0 \le t \le T} \sum_{k=0}^{\infty} \epsilon^{k+1} \|\hat{\partial}_t h_k(t)\|_{X_1}.$$
 (118)

Thus, by proving the boundedness of (118), we obtain the absolute convergence of (117) and, in particular, the existence of solutions to (51).

To obtain the required estimates, we first consider the truncated series (for $0 < k \le R$)

$$\sum_{j=0}^{R} \epsilon^{j+1} h_j(x_1, t).$$

Using (115), we have that

$$\begin{split} \|h_k(t)\|_{X_{R+1-k}} & \leq \sum_{\ell=-\infty}^{\infty} \frac{e^{(R+1-k)|\ell|}}{\sqrt{g|\ell|}} \int_0^t \left[\sum_{j=0}^{k-1} \sum_{m=-\infty}^{\infty} |\ell| |\partial_t \hat{h}_j(\ell-m,s)| |\partial_t \hat{h}_{k-1-j}(m,s)| \right. \\ & + 2g \sum_{j=0}^{k-1} \sum_{m=-\infty}^{\infty} |\ell| |\hat{h}_j(\ell-m,s)| |m| |\hat{h}_{k-1-j}(m,s)| \right] ds \\ & \leq \frac{1}{\sqrt{g}} \int_0^t \left[\sum_{j=0}^{k-1} \|\partial_t h_j(s)\|_{X_{R+2-k}} \|\partial_t h_{k-1-j}(s)\|_{X_{R+2-k}} \right. \\ & + 8g \sum_{j=0}^{k-1} \|h_j(s)\|_{X_{R+1.5-k}} \|h_{k-1-j}(s)\|_{X_{R+2-k}} \right] ds \\ & \leq \frac{1}{\sqrt{g}} \int_0^t \left[\sum_{j=0}^{k-1} \|\partial_t h_j(s)\|_{X_{R+2-k}} \|\partial_t h_{k-1-j}(s)\|_{X_{R+2-k}} \right] ds \\ & + 8g \sum_{j=0}^{k-1} \|h_j(s)\|_{X_{R+2-k}} \|h_{k-1-j}(s)\|_{X_{R+2-k}} \right] ds \,, \end{split}$$

where we have used Tonelli's theorem together with the fact that $\widehat{h_k}(0,t) = 0$, which follows from (113), and the important inequality

$$|\ell| \leqslant ce^{\frac{|\ell|}{c}} \leqslant ce^{\frac{|\ell-m|+|m|}{c}} \, \forall \, c \in \mathbb{Z}^+ \,.$$
 (119)

Using (116), we can find a similar bound $\partial_t h_k(t)$:

$$\|\partial_t h_k(t)\|_{X_{R+1-k}} \leq \frac{1}{\sqrt{g}} \int_0^t \left[\sum_{j=0}^{k-1} \|\partial_t h_j(s)\|_{X_{R+2-k}} \|\partial_t h_{k-1-j}(s)\|_{X_{R+2-k}} + 8g \sum_{j=0}^{k-1} \|h_j(s)\|_{X_{R+2-k}} \|h_{k-1-j}(s)\|_{X_{R+2-k}} \right] ds.$$

Since $R + 2 - k \le R + 2 - k + j = R + 1 - (k - 1 - j)$, it follows that

$$||u_{k-1-j}(s)||_{X_{R+2-k}} \le ||u_{k-1-j}(s)||_{X_{R+1-(k-1-j)}}$$

Similarly, if $j \le k-1$, then $R+2-k=R+1-(k-1) \le R+1-j$ and

$$||u_j(s)||_{X_{R+2-k}} \le ||u_j(s)||_{X_{R+1-j}}.$$

Then, we have that

$$\|h_{k}(t)\|_{X_{R+1-k}} + \|\partial_{t}h_{k}(t)\|_{X_{R+1-k}}$$

$$\leq \frac{2}{\sqrt{g}} \int_{0}^{t} \left[\sum_{j=0}^{k-1} \|\partial_{t}h_{j}(s)\|_{X_{R+2-k}} \|\partial_{t}h_{k-1-j}(s)\|_{X_{R+2-k}} \right] ds$$

$$+ 16g \sum_{j=0}^{k-1} \|h_{j}(s)\|_{X_{R+2-k}} \|h_{k-1-j}(s)\|_{X_{R+2-k}} \right] ds$$

$$\leq \frac{2}{\sqrt{g}} \int_{0}^{t} \left[\sum_{j=0}^{k-1} \|\partial_{t}h_{j}(s)\|_{X_{R+1-j}} \|\partial_{t}h_{k-1-j}(s)\|_{X_{R+1-(k-1-j)}} \right] ds$$

$$+ 16g \sum_{j=0}^{k-1} \|h_{j}(s)\|_{X_{R+1-j}} \|h_{k-1-j}(s)\|_{X_{R+1-(k-1-j)}} \right] ds$$

$$\leq \max \left\{ \frac{2}{\sqrt{g}}, 16g \right\} \int_{0}^{t} \left[\sum_{j=0}^{k-1} \|\partial_{t}h_{j}(s)\|_{X_{R+1-j}} \|\partial_{t}h_{k-1-j}(s)\|_{X_{R+1-(k-1-j)}} \right] ds . \tag{120}$$

$$+ \sum_{j=0}^{k-1} \|h_{j}(s)\|_{X_{R+1-j}} \|h_{k-1-j}(s)\|_{X_{R+1-(k-1-j)}} \right] ds .$$

We define

$$\mathscr{A}_k(t) = \max\left\{\frac{2}{\sqrt{g}}, 16g\right\} \left[\|h_k(t)\|_{X_{R+1-k}} + \|\partial_t h_k(t)\|_{X_{R+1-k}}\right], \text{ if } 1 \leqslant k, \ \mathscr{A}_0 = 1.$$

We then obtain that the previous recursion for $||h_k(t)||_{X_{R+1-k}} + ||\partial_t h_k(t)||_{X_{R+1-k}}$ can equivalently be stated as

$$\mathscr{A}_k(t) \leqslant \int_0^t \sum_{j=0}^{k-1} \mathscr{A}_{k-1-j}(s) \mathscr{A}_j(s) ds, \quad \mathscr{A}_0 = 1.$$

Then, we want to prove by induction that

$$\mathscr{A}_k \leqslant \mathcal{C}_k t^k \,, \tag{121}$$

where C_k are the Catalan numbers (64). Remarkably, the Catalan numbers $C_k = \mathcal{O}(k^{-\frac{3}{2}}4^k)$ as $k \to \infty$ [75, page 136].

Having already established that (121) holds for k = 0, we proceed with the induction

step. For $1 \leq k$, we have that

$$\mathscr{A}_{k}(s) \leqslant \int_{0}^{t} \sum_{j=0}^{k-1} \mathscr{A}_{k-1-j}(s) \mathscr{A}_{j}(s) ds$$

$$\leqslant \int_{0}^{t} \sum_{j=0}^{k-1} C_{k-1-j} s^{k-1-j} C_{j} s^{j} ds$$

$$\leqslant C_{k} \int_{0}^{t} s^{k-1} ds$$

$$\leqslant C_{k} \frac{t^{k}}{t}.$$

Thus, using the asymptotic growth of the Catalan numbers, we have that

$$||h_k(t)||_{X_1} + ||\partial_t h_k(t)||_{X_1} \le ||h_k(t)||_{X_{R+1-k}} + ||\partial_t h_k(t)||_{X_{R+1-k}} \le t^k 4^k.$$

Analogously,

$$||h_0(t)||_{X_1} + ||\partial_t h_0(t)||_{X_1} \le \widetilde{C}(||h_{\text{init}}||_{X_1}, ||\dot{h}_{\text{init}}||_{X_1}).$$

We define the series

$$I_R^1 = \partial_t h_0(x_1, t) + \epsilon \partial_t h_1(x_1, t) + \epsilon^2 \partial_t h_2(x_1, t) + \dots + \epsilon^R \partial_t h_R(x_1, t) ,$$

$$I_R^2 = h_0(x_1, t) + \epsilon h_1(x_1, t) + \epsilon^2 h_2(x_1, t) + \dots + \epsilon^R h_R(x_1, t) .$$

Then

$$||I_R^1||_{X_1} \leq \widetilde{C}(||h_{\text{init}}||_{X_1}, ||\dot{h}_{\text{init}}||_{X_1}) + \sum_{k=1}^R (\epsilon t 4)^k.$$

Similarly,

$$||I_R^2||_{X_1} \leqslant \widetilde{C}(||h_{\text{init}}||_{X_1}, ||\dot{h}_{\text{init}}||_{X_1}) + \sum_{k=1}^R (\epsilon t 4)^k.$$

We conclude that if

$$t<\frac{1}{\epsilon 4},$$

then we can take the limit in R and we compute that

$$\hat{\partial}_t h(x_1, t) = I_{\infty}^1$$
 and $h(x_1, t) = I_{\infty}^2$.

Our estimates lead to

$$h, \partial_t h \in L^{\infty}(0, T; X_1).$$

Moreover, using the Cauchy product of power series, we have that

$$\hat{h}(\ell,t) = \hat{h}_0(\ell,0)\cos\left(\sqrt{g|\ell|}t\right) + \hat{\sigma}_t\hat{h}_0(\ell,0)\sin\left(\sqrt{g|\ell|}t\right) + \frac{1}{\sqrt{g|\ell|}}\int_0^t \mathcal{N}(\ell,s)\sin\left(\sqrt{g|\ell|}(t-s)\right)ds,$$

$$\hat{\sigma}_t\hat{h}(\ell,t) = -\hat{h}_0(\ell,0)\sin\left(\sqrt{g|\ell|}t\right) + \hat{\sigma}_t\hat{h}_0(\ell,0)\cos\left(\sqrt{g|\ell|}t\right) + \int_0^t \mathcal{N}(\ell,s)\cos\left(\sqrt{g|\ell|}(t-s)\right)ds,$$

where

$$\mathcal{N}(\ell,t) = \sum_{m=-\infty}^{\infty} \left[-|\ell| \left((-i \operatorname{sgn}(\ell-m)) \, \partial_t \hat{h}(\ell-m,t) \, (-i \operatorname{sgn}(m)) \, \partial_t \hat{h}(m,t) \right) + g \left(i \ell \hat{h}(\ell-m,t) i m \hat{h}(m,t) + |\ell| \hat{h}(\ell-m,t) |m| \hat{h}(m,t) \right) \right].$$

Since h and $\partial_t h$ are analytic functions in space, using the previous expression, we obtain that h and $\partial_t h$ satisfy

$$h, \partial_t h \in C([0, T], X_{0.5}).$$

In particular, they are continuous functions in time, $h, \partial_t h \in C([0,T] \times \mathbb{S}^1)$.

Uniqueness. Let us assume that there exist two solutions $h^{(1)}, h^{(2)} \in C([0, T], X_{0.5})$ emanating from the same initial data. Then, the difference

$$z = h^{(1)} - h^{(2)}$$

satisfies

$$\widehat{z}(\ell,t) = \frac{1}{\sqrt{g|\ell|}} \int_0^t \mathcal{M}(\ell,s) \sin\left(\sqrt{g|\ell|}(t-s)\right) ds,$$

$$\partial_t \widehat{z}(\ell,t) = \int_0^t \mathcal{M}(\ell,s) \cos\left(\sqrt{g|\ell|}(t-s)\right) ds,$$

with

$$\mathcal{M}(\ell,t) = \sum_{m=-\infty}^{\infty} \left[-|\ell| \left((-i\mathrm{sgn}(\ell-m)) \, \partial_t \widehat{z}(\ell-m,t) \, (-i\mathrm{sgn}(m)) \, \partial_t \widehat{h}^{(1)}(m,t) \right) \right.$$

$$\left. -|\ell| \left((-i\mathrm{sgn}(\ell-m)) \, \partial_t \widehat{h}^{(2)}(\ell-m,t) \, (-i\mathrm{sgn}(m)) \, \partial_t \widehat{z}(m,t) \right) \right.$$

$$\left. + g \left(i\ell \widehat{z}(\ell-m,t) im \widehat{h}^{(1)}(m,t) + |\ell| \widehat{z}(\ell-m,t) |m| \widehat{h}^{(1)}(m,t) \right) \right.$$

$$\left. + g \left(i\ell \widehat{h}^{(2)}(\ell-m,t) im \widehat{z}(m,t) + |\ell| \widehat{h}^{(2)}(\ell-m,t) |m| \widehat{z}(m,t) \right) \right].$$

Then, following the same argument as in the previous section, we expand $h_k^{(j)}$, j = 1, 2 as in (114) and find that $h_k^{(j)}$, j = 1, 2 satisfy the cascade of linear problems (111) and (112). Equivalently, we have that

$$z_k = h_k^{(1)} - h_k^{(2)},$$

satisfies

$$\begin{split} \widehat{z}_k(\ell,t) &= \frac{1}{\sqrt{g|\ell|}} \int_0^t f_k(\ell,s) \sin\left(\sqrt{g|\ell|}(t-s)\right) \, ds \,, \\ \widehat{c}_t \widehat{z}_k(\ell,t) &= \int_0^t f_k(\ell,s) \cos\left(\sqrt{g|\ell|}(t-s)\right) \, ds \,, \end{split}$$

with

$$f_{k}(\ell,t) = \sum_{j=0}^{k-1} \sum_{m=-\infty}^{\infty} \left[-|\ell| \left((-i\mathrm{sgn}(\ell-m)) \, \hat{\partial}_{t} \hat{z}_{j}(\ell-m,t) \, (-i\mathrm{sgn}(m)) \, \hat{\partial}_{t} \hat{h}_{k-1-j}^{(1)}(m,t) \right) \right.$$

$$\left. - |\ell| \left((-i\mathrm{sgn}(\ell-m)) \, \hat{\partial}_{t} \hat{h}_{k-1-j}^{(2)}(\ell-m,t) \, (-i\mathrm{sgn}(m)) \, \hat{\partial}_{t} \hat{z}_{j}(m,t) \right) \right.$$

$$\left. + g \left(i\ell \hat{z}_{j}(\ell-m,t) im \hat{h}_{k-1-j}^{(1)}(m,t) + |\ell| \hat{z}_{j}(\ell-m,t) |m| \hat{h}_{k-1-j}^{(1)}(m,t) \right) \right.$$

$$\left. + g \left(i\ell \hat{h}_{k-1-j}^{(2)}(\ell-m,t) im \hat{z}_{j}(m,t) + |\ell| \hat{h}_{k-1-j}^{(2)}(\ell-m,t) |m| \hat{z}_{j}(m,t) \right) \right].$$

As before, we consider $R \in \mathbb{Z}^+$ and define

$$\mathscr{A}_{k}^{(1)}(t) = \max\left\{\frac{2}{\sqrt{g}}, 16g\right\} \left[\|h_{k}^{(1)}(t)\|_{X_{R+1-k}} + \|\partial_{t}h_{k}^{(1)}(t)\|_{X_{R+1-k}} \right], \, \mathscr{A}_{0}^{(1)} = 1,$$

$$\mathscr{A}_{k}^{(2)}(t) = \max\left\{\frac{2}{\sqrt{g}}, 16g\right\} \left[\|h_{k}^{(2)}(t)\|_{X_{R+1-k}} + \|\partial_{t}h_{k}^{(2)}(t)\|_{X_{R+1-k}} \right], \, \mathscr{A}_{0}^{(2)} = 1,$$

$$\mathscr{B}_{k}(t) = \max\left\{\frac{2}{\sqrt{g}}, 16g\right\} \left[\|z_{k}(t)\|_{X_{R+1-k}} + \|\partial_{t}z_{k}(t)\|_{X_{R+1-k}} \right].$$

Following the arguments in the previous section, we find that

$$\mathscr{A}_k^{(j)} \leqslant \mathcal{C}_k t^k, \ j = 1, 2$$

$$\mathscr{B}_k(t) \leqslant \int_0^t \sum_{j=0}^{k-1} \left(\mathscr{A}_{k-1-j}^{(1)}(s) + \mathscr{A}_{k-1-j}^{(2)}(s) \right) \mathscr{B}_j(s) \, ds,$$

$$\mathscr{B}_0(t) = 0.$$

Due to the previous inequalities, we prove that $\mathcal{B}_k(t) = 0$ using induction and we conclude the uniqueness.

References

- [1] George Biddell Airy. Tides and waves. 1841. 1
- [2] Benjamin Akers and Paul A. Milewski. Dynamics of three-dimensional gravity-capillary solitary waves in deep water. SIAM J. Appl. Math., 70(7):2390–2408, 2010. 1, 5.2, 7
- [3] Benjamin Akers and David P Nicholls. Traveling waves in deep water with gravity and surface tension. SIAM Journal on Applied Mathematics, 70(7):2373–2389, 2010. 1, 1, 5.2
- [4] Benjamin Akers and David P Nicholls. Spectral stability of deep two-dimensional gravity water waves: repeated eigenvalues. SIAM Journal on Applied Mathematics, 72(2):689–711, 2012. 1

- [5] Benjamin Akers and David P. Nicholls. The spectrum of finite depth water waves. Eur. J. Mech. B Fluids, 46:181–189, 2014. 1
- [6] Thomas Alazard, Nicolas Burq, and Claude Zuily. On the cauchy problem for gravity water waves. *Inventiones mathematicae*, 198(1):71–163, 2014. 1
- [7] Thomas Alazard and Jean-Marc Delort. Global solutions and asymptotic behavior for two dimensional gravity water waves. Ann. Sci. Éc. Norm. Supér.(4), 48(5):1149–1238, 2015. 1
- [8] Borys Alvarez-Samaniego and David Lannes. Large time existence for 3D water-waves and asymptotics. *Invent. Math.*, 171(3):485–541, 2008. 1
- [9] D. M. Ambrose and J. Wilkening. On ill-posedness of truncated series models for water waves *Proc. R. Soc. A*, 470(2166):20130849, 2014. 7
- [10] D. M. Ambrose and J. Wilkening. Computation of symmetric, time-periodic solutions of the vortex sheet with surface tension. *Proc. Nat. Acad. Sci.*, 107(8):3361–3366, 2010. 9.3
- [11] D. M. Ambrose and J. Wilkening. Dependence of time-periodic votex sheets with surface tension on mean vortex sheet strength. *Procedia IUTAM*, 11:15–22, 2014. 9.3
- [12] David M. Ambrose and Nader Masmoudi. The zero surface tension limit of two-dimensional water waves. Comm. Pure Appl. Math., 58(10):1287–1315, 2005. 1
- [13] C. J. Amick and J. F. Toland. The semi-analytic theory of standing waves. *Proc. Roy. Soc. Lond. A*, 411:123–138, 1987. 9.3
- [14] J. Thomas Beale, Thomas Y. Hou, and John Lowengrub. Convergence of a boundary integral method for water waves. SIAM J. Numer. Anal., 33(5):1797–1843, 1996. 1
- [15] D. J. Benney and J. C. Luke. On the interactions of permanent waves of finite amplitude. Stud. Appl. Math., 43:309–313, 1964. 1
- [16] K. M. Berger and P. A. Milewski. Simulation of wave interactions and turbulence in one-dimensional water waves. SIAM J. Appl. Math., 63(4):1121–1140, 2003. 1
- [17] Joseph Boussinesq. Théorie des ondes et des remous qui se propagent le long d'un canal rectangulaire horizontal, en communiquant au liquide contenu dans ce canal des vitesses sensiblement pareilles de la surface au fond. *Journal de Mathématiques Pures et Appliquées*, pages 55–108, 1872. 1
- [18] Joseph Boussinesq. Essai sur la théorie des eaux courantes. Imprimerie nationale, 1877.
- [19] A. Castro, D. Córdoba, C.L. Fefferman, F. Gancedo, and J. Gómez-Serrano. Splash singularity for water waves. *Proceedings of the National Academy of Sciences*, 109(3):733– 738, 2012. 9.3

- [20] Angel Castro, Diego Córdoba, Charles Fefferman, Francisco Gancedo, and Javier Gómez-Serrano. Finite time singularities for the free boundary incompressible Euler equations. *Ann. of Math.* (2), 178(3):1061–1134, 2013. 1
- [21] J. Chen and J. Wilkening. Arbitrary-order exponential time differencing schemes via Chebyshev moments of exponential functions. 2019. (in preparation). 1, 9.2, 9.2
- [22] C. H. Arthur Cheng, Daniel Coutand, and Steve Shkoller. On the limit as the density ratio tends to zero for two perfect incompressible fluids separated by a surface of discontinuity. *Comm. Partial Differential Equations*, 35(5):817–845, 2010. 1
- [23] C. H. Arthur Cheng and Steve Shkoller. Solvability and Regularity for an Elliptic System Prescribing the Curl, Divergence, and Partial Trace of a Vector Field on Sobolev-Class Domains. J. Math. Fluid Mech., 19(3):375–422, 2017. 3.3
- [24] Ching-Hsiao Arthur Cheng, Daniel Coutand, and Steve Shkoller. On the motion of vortex sheets with surface tension in three-dimensional Euler equations with vorticity. *Comm. Pure Appl. Math.*, 61(12):1715–1752, 2008. 1
- [25] W. Choi. Nonlinear evolution equations for two-dimensional surface waves in a fluid of finite depth. J. Fluid Mech. 295:381, 1995. 1
- [26] Daniel Coutand and Steve Shkoller. Well-posedness of the free-surface incompressible Euler equations with or without surface tension. J. Amer. Math. Soc., 20(3):829–930, 2007. 1
- [27] Daniel Coutand and Steve Shkoller. On the finite-time splash and splat singularities for the 3-d free-surface euler equations. *Communications in Mathematical Physics*, 325(1):143–183, 2014. 1, 9.3
- [28] Daniel Coutand and Steve Shkoller. On the impossibility of finite-time splash singularities for vortex sheets. Arch. Ration. Mech. Anal., 221(2):987–1033, 2016. 1
- [29] S. M. COX and P. C. Matthews. Exponential time differencing for stiff systems. *J. Comput. Phys.*, 176:430–455, 2002. 1, 9.2
- [30] Walter Craig. An existence theory for water waves and the Boussinesq and Korteweg-de Vries scaling limits. Comm. Partial Differential Equations, 10(8):787–1003, 1985. 1
- [31] Walter Craig and Catherine Sulem. Numerical simulation of gravity waves. *Journal of Computational Physics*, 108(1):73–83, 1993. 1, 7
- [32] Y Deng, AD Ionescu, B Pausader, and F Pusateri. Global solutions of the gravity-capillary water wave system in 3 dimensions. *Acta Mathematica*, 219:213–402, 2017.
- [33] A. L. Dyachenko, E. A. Kuznetsov, M. D. Spector, and V. E. Zakharov. Analytic description of the free surface dynamics of an ideal fluid (canonical formalism and conformal mapping). *Phys. Lett. A*, 221:73–79, 1996. 9.1

- [34] A. L. Dyachenko, V. E. Zakharov, and E. A. Kuznetsov. Nonlinear dynamics on the free surface of an ideal fluid. *Plasma Phys. Rep.*, 22:916–928, 1996. 9.1
- [35] Charles Fefferman, Alexandru D. Ionescu, and Victor Lie. On the absence of splash singularities in the case of two-fluid interfaces. *Duke Math. J.*, 165(3):417–462, 2016. 1
- [36] Gerald B. Folland. *Introduction to Partial Differential Equations*. Princeton University Press, Princeton, 1995. 9.1
- [37] P. Germain, Nader Masmoudi, and Jalal Shatah. Global solutions for the gravity water waves equation in dimension 3. Ann. of Math. (2), 175:691–754, 2012. 1
- [38] R. Granero-Belinchón and S. Shkoller. A model for Rayleigh-Taylor mixing and interface turnover. *Multiscale Model. Simul.*, 15:274–308, 2017. 1, 5.2, 6
- [39] Ernst Hairer, Syvert P. Norsett, and Gerhard Wanner. Solving Ordinary Differential Equations I: Nonstiff Problems. Springer, Berlin, 2nd edition, 2000. 9.1, 9.2, 9.3
- [40] T. Y. Hou and R. Li. Computing nearly singular solutions using pseudo-spectral methods. J. Comput. Phys., 226:379–397, 2007. 9.3
- [41] T. Y. Hou, J. S. Lowengrub, and M. J. Shelley. Removing the stiffness from interfacial flows with surface tension. *J. Comput. Phys.*, 114:312–338, 1994. 9.3
- [42] T. Y. Hou, J. S. Lowengrub, and M. J. Shelley. The long-time motion of vortex sheets with surface tension. *Phys. Fluids*, 9:1933–1954, 1997. 9.3
- [43] T. Y. Hou, J. S. Lowengrub, and M. J. Shelley. Boundary integral methods for multicomponent fluids and multiphase materials. J. Comput. Phys., 169:302–362, 2001. 9.3
- [44] John K Hunter, Mihaela Ifrim, and Daniel Tataru. Two dimensional water waves in holomorphic coordinates. *Communications in Mathematical Physics*, 346(2):483–552, 2016. 1
- [45] Mihaela Ifrim and Daniel Tataru. Two dimensional water waves in holomorphic coordinates ii: global solutions. arXiv preprint arXiv:1404.7583, 2014. 1
- [46] Alexandru D Ionescu and Fabio Pusateri. Global solutions for the gravity water waves system in 2d. *Inventiones mathematicae*, 199(3):653–804, 2015. 1
- [47] G. Iooss, P. I. Plotnikov, and J. F. Toland. Standing waves on an infinitely deep perfect fluid under gravity. *Arch. Rat. Mech. Anal.*, 177:367–478, 2005. 9.3
- [48] Aly-Khan Kassam and Lloyd N. Trefethen. Fourth-order time-stepping for stiff pdes. SIAM J. Sci. Comput., 26:1214–1233, 2006. 1, 9.2
- [49] George Knightly. On a class of global solutions of the Navier-Stokes equations. Arch. Ration. Mech. Anal., 21(3):211–245, 1966. 6

- [50] David Lannes. Well-posedness of the water-waves equations. J. Amer. Math. Soc., 18(3):605–654, 2005. 1
- [51] David Lannes and Philippe Bonneton. Derivation of asymptotic two-dimensional time-dependent equations for surface water wave propagation. *Physics of Fluids*, 21:1–9, 2009. 1
- [52] Hans Lindblad. Well-posedness for the motion of an incompressible liquid with free surface boundary. Ann. of Math. (2), 162(1):109–194, 2005. 1
- [53] Y Matsuno. Nonlinear Evolutions of Surface Gravity Waves on Fluid of Finite Depth. *Phys. Rev. Let.*, 69(4):609–611, 1992. 1
- [54] Y Matsuno. Nonlinear evolution of surface gravity waves over an uneven bottom. J. Fluid Mech., 249:121–133, 1993. 1
- [55] Y Matsuno. Two-dimensional evolution of surface gravity waves on a fluid of arbitrary depth. *Phys. Rev. E*, 47(6):4593–4596, 1993. 1
- [56] D Michael Milder. An improved formalism for wave scattering from rough surfaces. The Journal of the Acoustical Society of America, 89(2):529–541, 1991. 3
- [57] D Michael Milder and H Thomas Sharp. An improved formalism for rough-surface scattering. ii: Numerical trials in three dimensions. *The Journal of the Acoustical Society of America*, 91(5):2620–2626, 1992. 3
- [58] P. A. Milewski, J.-M. Vanden-Broeck, and Z. Wang. Dynamics of steep two-dimensional gravity-capillary solitary waves. *J. Fluid Mech.*, 664:466–477, 2010. 9.1
- [59] N. I. Muskhelishvili. Singular Integral Equations. Dover Publications, Inc., New York, 2nd edition, 1992. 9.1
- [60] VI Nalimov. The cauchy-poisson problem. Dinamika Splovsn. Sredy, (Vyp. 18 Dinamika Zidkost. so Svobod. Granicami), 254:104–210, 1974. 1
- [61] David P. Nicholls and Fernando Reitich. On analyticity of travelling water waves. Proc. R. Soc. Lond. Ser. A Math. Phys. Eng. Sci., 461(2057):1283–1309, 2005.
- [62] David P. Nicholls and Fernando Reitich. Stable, high-order computation of traveling water waves in three dimensions. Eur. J. Mech. B Fluids, 25(4):406–424, 2006. 1
- [63] L. Nirenberg. An abstract form of the nonlinear Cauchy-Kowalewski theorem. J. Differential Geometry, 6:561–576, 1972. 6
- [64] T. Nishida. A note on a theorem of Nirenberg. J. Differential Geometry, 12:629–633, 1977. 6
- [65] C. W. Oseen. Sur les formules de green généralisées qui se présentent dans l'hydrodynamique et sur quelquesunes de leurs applications. *Acta Mathematica*, 35(1):97–192, 1912. 6

- [66] LV Ovsjannikov. Shallow-water theory foundation. Archives of Mechanics, 26(3):407–422, 1974. 8, 8
- [67] LV Ovsjannikov. Cauchy problem in a scale of Banach spaces and its application to the shallow water theory justification Applications of methods of functional analysis to problems in mechanics, 426–437, 1976. 6
- [68] W G Penney and A T Price. Finite periodic stationary gravity waves in a perfect liquid, part II. *Phil. Trans. R. Soc. London A*, 244:254–284, 1952. 9.3
- [69] P.J. Prince and J.R. Dormand. High order embedded Runge-Kutta formulae. J. Comp. Appl. Math., 7:67–75, 1981. 9.1, 9.3
- [70] B. Rayleigh. On waves. Philos. Mag., 1:257–279, 1876. 9.3
- [71] Guido Schneider and Eugene C. Wayne, Justification of the NLS approximation for a quasilinear water wave model *Journal of Differential Equations*, 251(2):238–269, 2011. 6, 6.1
- [72] L. W. Schwartz and A. K. Whitney. A semi-analytic solution for nonlinear standing waves in deep water. *J. Fluid Mech.*, 107:147–171, 1981. 9.3
- [73] Jalal Shatah and Chongchun Zeng. Local well-posedness for fluid interface problems. Archive for Rational Mechanics and Analysis, 199(2):653–705, 2011. 1
- [74] Marvin Shinbrot. The initial value problem for surface waves under gravity, i: the simplest case. *Indiana University Mathematics Journal*, 25(3):281–300, 1976. 8, 8
- [75] Richard P Stanley. Catalan numbers. Cambridge University Press, 2015. 1, B
- [76] George G Stokes. On the theory of oscillatory waves. Trans Cambridge Philos Soc, 8:441–473, 1847. 1
- [77] I Tadjbakhsh and J B Keller. Standing surface waves of finite amplitude. J. Fluid Mech., 8:442–451, 1960. 9.3
- [78] J. Wilkening. Breakdown of self-similarity at the crests of large amplitude standing water waves. *Phys. Rev. Lett*, 107:184501, 2011. 9.1, 9.3
- [79] J. Wilkening and J. Yu. Overdetermined shooting methods for computing standing water waves with spectral accuracy. *Computational Science & Discovery*, 5:014017, 2012. 9.1, 9.1, 9.3, 9.3, 9.3
- [80] Sijue Wu. Well-posedness in Sobolev spaces of the full water wave problem in 2-D. *Invent. Math.*, 130(1):39–72, 1997. 1
- [81] Sijue Wu. Almost global wellposedness of the 2-D full water wave problem. *Invent.* Math., 177(1):45–135, 2009. 1

- [82] Sijue Wu. Global wellposedness of the 3-D full water wave problem. Invent. Math., $184(1):125-220,\ 2011.\ 1$
- [83] Hideaki Yosihara. Gravity waves on the free surface of an incompressible perfect fluid of finite depth. *Publications of the Research Institute for Mathematical Sciences*, 18(1):49–96, 1982. 1
- [84] Vladimir E Zakharov. Stability of periodic waves of finite amplitude on the surface of a deep fluid. Journal of Applied Mechanics and Technical Physics, 9(2):190–194, 1968. 7